

Theory for Anomalous NMR Response in $\text{Pb}_{1-x}\text{Tl}_x\text{Te}$ on Charge Kondo Effect

Kazumasa Miyake^{1*} and Hiroyasu Matsuura²

¹ Center for Advanced High Magnetic Field Science, Osaka University, Toyonaka, Osaka 560-0043, Japan

² Department of Physics, University of Tokyo, Hongo, Bunkyo-ku, Tokyo 113-0033, Japan

(Received March 1, 2022)

A theory for anomalous enhancement of NMR relaxation rate $1/T_1T$ of ^{125}Te toward zero temperature observed in $\text{Pb}_{1-x}\text{Tl}_x\text{Te}$ ($x=0.01$) is presented on the idea of the charge Kondo effect of valence skipping element Tl. It is found that such enhancement in $1/T_1T$ is caused through enhancement of the pair-hopping and inter-orbital interactions between 6s electrons localized on Tl site and conduction electrons doped in the hole band the semiconductor PbTe, which is the heart of the charge Kondo effect. It is also found that the Knight shift K is enhanced in proportion to the increasing part of the relaxation rate $1/T_1T$ in the same temperature region, implying that the Korringa relation does not hold in such a region of temperature.

1. Introduction

In the past decade, valence skipping phenomenon and related superconductivity have caused revived attention since the charge Kondo effect and the superconductivity had been reported in $\text{Pb}_{1-x}\text{Tl}_x\text{Te}$ ($0.006 < x < 0.015$).¹⁾ Since the valence state of Pb is Pb^{2+} , the nominal valence of Tl should be Tl^{2+} . However, the doped atom Tl is known as a valence skipping element which takes Tl^{1+} [(6s)⁰ configuration] or Tl^{3+} [(6s)² configuration] but not Tl^{2+} , implying that (6s)¹ configuration is skipped even though a nominal valence is Tl^{2+} as in a series of compounds.²⁾ The logarithmic temperature dependence in the resistivity $\rho(T)$ in the low temperature region ($T < 10\text{K}$), which is robust against the magnetic field, and the occurrence of superconductivity were shown to be well explained on the basis of the negative- U Anderson model,³⁾ while fundamental properties of the negative- U Anderson model had already been derived in the beginning of 1990s.⁴⁾

Recently, it has been shown by the numerical renormalization group (NRG) calculation that the pair-hopping interaction U_{ph} between the localized electron and extended conduction electrons can give rise to the negative- U or valence skipping effect and the charge Kondo effect simultaneously.⁵⁾ More explicitly, it was shown that there exist two temperature (energy) scales T^* and T_K ($T_K < T^*$), with T_K being the Kondo temperature of the present problem, i.e., at $T < T^*$, (6s)¹ state is excluded (skipped) and (6s)⁰ and (6s)² states are degenerate or the negative- U effect manifests itself, and at

*miyake@toyotariken.jp

$T \lesssim T_K$, the charge Kondo effect occurs forming the charge singlet state, like the Kondo-Yosida spin singlet state. This origin of negative- U effect was new and quite different from a series of proposals which had already been given,⁶⁻¹¹⁾ while its origin still remains as an active subject.¹²⁾ Since there exists no magnetic ions in Tl doped PbTe, it is reasonable to expect that the two-fold charge degrees of freedom of Tl ion, Tl^{1+} and Tl^{3+} , is the origin of Kondo like behavior in the resistivity so that it was called the charge Kondo effect.^{1,3,4)}

Quite recently, temperature dependence of NMR relaxation rates $1/T_1T$ of ^{125}Te of $\text{Pb}_{1-x}\text{Tl}_x\text{Te}$ were reported to exhibit diverging increase below $T = 10$ K for the sample $x \simeq 0.01$ [ref. 13] which shows the charge Kondo effect in the resistivity and the superconductivity in the lower temperature region $T \lesssim T_K$.¹⁾ This is non-trivial because elements consisting of this compound are all non-magnetic ones, which suggests that the enhancement of $1/T_1T$ may give another smoking gun for the valence skipping or the negative- U effect to play a crucial role in this compound.

The purpose of the present paper is to clarify how the charge Kondo effect can give rise to the diverging behavior in $1/T_1T$ across the Kondo temperature T_K , reinforcing that the charge Kondo effect is the origin of anomalous properties observed in $\text{Pb}_{1-x}\text{Tl}_x\text{Te}$ ($0.006 < x < 0.015$). Organization of the paper is as follows. In Sect. 2, a formulation for discussing the relaxation rate $1/T_1T$ is given on the basis of the charge Kondo effect due to the pair-hopping interaction U_{ph} . In Sect. 3.1, it is shown the anomalous behaviors in the $1/T_1T$ arises from the first order process in the renormalized pair-hopping interaction $U_{\text{ph}}(T)$ by the charge Kondo effect at $T \gtrsim T_K$. In Sect. 3.2, it is also shown that the $1/T_1T$ is similarly influenced by the renormalized inter-orbital interaction $U_{\text{dc}}(T)$ between the localized electron and extended conduction electrons. As a result, it is shown in Sect. 3.3 that the anomalous temperature dependence of $1/T_1T$ observed in $\text{Pb}_{1-x}\text{Tl}_x\text{Te}$ ($x = 0.01$) is explained by these effects. In Sect. 4, it is shown that the charge Kondo effect also gives an enhancement of the Knight shift K in proportion to that of $1/T_1T$, implying that the Korringa relation is apparently broken where the relaxation rate is enhanced by its effect.

2. Formulation

An effective model including the Coulomb interaction between the conduction electron and localized 6s orbital (denoted by d for manifesting the relation with the s-d model) is given by as⁵⁾

$$\mathcal{H}_0 = \mathcal{H}_c + \mathcal{H}_d + \mathcal{H}_{\text{dc}} + \mathcal{H}_{\text{ph}} + \mathcal{H}_{\text{hyb}}, \quad (1)$$

where the first term is for the conduction electron, the second term is for 6s electrons, and the third and fourth terms are for the Coulomb interactions U_{dc} and the pair-hopping interaction U_{ph} between

conduction electron and localized 6s electrons. Explicit expression of these terms are given as

$$\mathcal{H}_c \equiv \frac{1}{N} \sum_{\mathbf{k}\sigma} \epsilon_{\mathbf{k}} c_{\mathbf{k}\sigma}^\dagger c_{\mathbf{k}\sigma}, \quad (2)$$

$$\mathcal{H}_d \equiv \epsilon_d \sum_{\sigma} n_{d\sigma}, \quad (3)$$

$$\mathcal{H}_{dc} \equiv U_{dc} \frac{1}{N} \sum_{\mathbf{k}\sigma} c_{\mathbf{k}\sigma}^\dagger c_{\mathbf{k}\sigma} n_{d\sigma'}, \quad (4)$$

$$\mathcal{H}_{ph} \equiv U_{ph} \frac{1}{N} \sum_{\mathbf{k}\mathbf{k}'} \left(d_{\uparrow}^\dagger d_{\downarrow}^\dagger c_{\mathbf{k}\downarrow} c_{\mathbf{k}'\uparrow} + \text{h.c.} \right), \quad (5)$$

$$\mathcal{H}_{hyb} \equiv V_{dc} \frac{1}{\sqrt{N}} \sum_{\mathbf{k}\sigma} \left(c_{\mathbf{k}\sigma}^\dagger d_{\sigma} + \text{h.c.} \right), \quad (6)$$

where N is the number of lattice sites, and $n_{d\sigma} \equiv d_{\sigma}^\dagger d_{\sigma}$ is the number operator of the localized 6s electrons. Hereafter, the origin of energy is taken as the Fermi energy of conduction electrons ϵ_F , the chemical potential at $T = 0$, and the temperature T is assumed to be low enough compared to ϵ_F , i.e., $k_B T \ll \epsilon_F$.

As discussed in Ref. 5, the pair-hopping interaction U_{ph} can stabilize the valence skipping state and cause the charge Kondo effect under certain condition. The origin of this phenomenon can be understood intuitively if we note that the U_{ph} is transformed to the pseudo-spin flipping exchange interaction (the origin of the Kondo effect) by the particle-hole transformation for the annihilation operators d_{\downarrow} and $c_{\mathbf{k}\downarrow}$ as shown explicitly in Appendix.

The NMR relaxation rate $1/T_1$ is given by the Moriya formula as¹⁴⁾

$$\frac{1}{T_1 T} = A^2 \frac{1}{\omega} \text{Im} \Gamma^R(\omega + i\delta), \quad (7)$$

where A is the hyper-fine coupling constant between electron and nuclei, and $\Gamma(i\omega_{\nu})$ is the transverse spin susceptibility of conduction electrons at certain Te site where NMR relaxation is observed and has several contributions, in general. The $\Gamma_{ph}(i\omega)$ arising from the lowest order process in U_{ph} is given by the Feynman diagram shown in Fig. 1 and its vertical inversion as follows:

$$\begin{aligned} \Gamma_{ph}(i\omega_{\nu}) &= 2V_{dc}^2 T^2 \sum_{\epsilon_n} U_{ph} G_c(\mathbf{r}_{ij}, i\epsilon_n) G_c(\mathbf{r}_{ij}, i\epsilon_n + i\omega_{\nu}) G_c(\mathbf{r}_{ij}, -i\epsilon_n) G_c(\mathbf{r}_{ij}, -i\epsilon_n + i\omega_{\nu}) \\ &\quad \times G_d(-i\epsilon_n + i\omega_{\nu}) G_d(i\epsilon_n), \end{aligned} \quad (8)$$

where we have used the property $G_c(-\mathbf{r}_{ij}, i\epsilon_n) = G_c(\mathbf{r}_{ij}, i\epsilon_n)$ etc., and the factor 2 arises from the diagrams of the vertical inversion.

The expression [Eq. 8] is verified by the Wick decomposition as

$$\left\langle T_{\tau} \left[\bar{c}_{i\uparrow}(\tau) c_{i\downarrow}(\tau) (-U_{ph}) \bar{d}_{j\uparrow}(\tau') \bar{d}_{j\downarrow}(\tau') c_{j\downarrow}(\tau') c_{j\uparrow}(\tau') \bar{c}_{i\downarrow}(\tau'') c_{i\uparrow}(\tau'') \right] \right\rangle$$

$$= U_{\text{ph}} \langle T_{\tau} c_{j\uparrow}(\tau') \bar{c}_{i\uparrow}(\tau) \rangle \langle T_{\tau} c_{j\downarrow}(\tau') \bar{c}_{i\downarrow}(\tau'') \rangle \langle T_{\tau} c_{i\downarrow}(\tau) \bar{d}_{j\downarrow}(\tau') \rangle \langle T_{\tau} c_{i\uparrow}(\tau'') \bar{d}_{j\uparrow}(\tau') \rangle \quad (9)$$

The reason why the Green functions with $\mp i\varepsilon_n$ and $\pm i\varepsilon_n + i\omega_\nu$ are paired in Fig. 1 is based on the fact that the Kondo-like renormalization enhancing the pair-hopping interaction U_{ph} arises for the annihilation process of pair of conduction electrons with $i\varepsilon_n$ and $-i\varepsilon_n$ as discussed in Appendix. Namely, the expression [Eq. (8)] is regarded as the most divergent part when U_{ph} divergently grows for the elastic scattering channel by the charge Kondo effect as decreasing temperature. This treatment of extracting the most divergent contribution is analogous to that adopted in the problem of estimating the effect of superconducting fluctuations to the conductivity near the superconducting transition point.^{15–17)} The renormalization of U_{ph} for a specified localized electron arises through the higher order terms in U_{ph} as in the conventional Kondo effect, and can be performed by the renormalization group (RG) method such as the poorman's scaling approach as discussed below.¹⁹⁾ On the other hand, the higher order terms in U_{ph} among different localized electrons are higher order in the impurity concentration and are safely neglected in the present case where the concentration of Tl impurity is small about 10^{-2} .

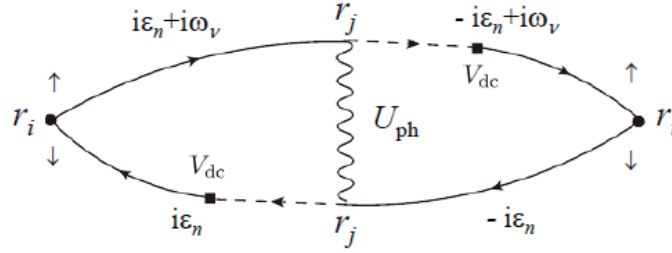


Fig. 1. Feynman diagram giving the NMR longitudinal relaxation rates $1/T_1T$ at Te (\mathbf{r}_i) site in the lowest order with respect to the pair-hopping interaction U_{ph} . Wavy line represents U_{ph} at Tl (\mathbf{r}_j) site. Solid lines with arrow and dashed lines with arrow represent the Matsubara Green function of conduction electrons of conduction band (in hole picture) and 6s electron at Tl site, respectively. Filled squares represent the hybridization V_{dc} between conduction electrons and 6s electron at Tl site.

As shown in Appendix, the Green function of the conduction electrons $G_c(\mathbf{r}, i\varepsilon_n)$ is expressed by a spectral representation as

$$G_c(\mathbf{r}, i\varepsilon_n) = \int_{-\infty}^{\infty} dy \frac{\rho(\mathbf{r}, y)}{i\varepsilon_n - y}, \quad (10)$$

with a spectral function

$$\rho(\mathbf{r}, y) = N_F \frac{e^{-(r/2\ell)}}{k_{\text{F}r}} \sin \left[\sqrt{\frac{y}{\epsilon_{\text{F}}} + 1} (k_{\text{F}r}) \right] \theta(y + \epsilon_{\text{F}}) \theta(\epsilon_{\text{c}} - y), \quad (11)$$

where $N_F \equiv mk_{\text{F}}/2\pi^2N$ is the density of states of conduction electrons at the Fermi level, per lattice

site and spin component, and ϵ_F and ϵ_c are the Fermi energy of conduction electrons and the energy cutoff of the conduction band in the hole (check) picture and a mean-free path due to the impurity scattering,²⁴⁾ respectively. In the limit $k_F r \ll 1$, the spectral function takes a form as

$$\rho(\mathbf{r}, y) \approx N_F e^{-(r/2\ell)} \sqrt{\frac{y}{\epsilon_F} + 1} \theta(y + \epsilon_F) \theta(\epsilon_c - y). \quad (12)$$

The Green function of localized electron at valence-skipping site, i.e., T1 site, is given by

$$G_d(i\epsilon_n) = \frac{1}{i\epsilon_n - \epsilon_d} \quad (13)$$

where ϵ_d is the energy level of localized electron measured from the chemical potential.

3. NMR Relaxation Rate at $T \gtrsim T_K$

3.1 Effect of pair-hopping interaction

In this subsection, the NMR relaxation rate triggered by the pair-hopping interaction U_{ph} . As shown in Appendix, $\text{Im}\Gamma^{\text{R}}(\omega + i\delta)$ is given by

$$\begin{aligned} \text{Im}\Gamma_{\text{ph}}^{\text{R}}(\omega + i\delta) = & -\frac{2\pi V_{\text{dc}}^2 T U_{\text{ph}}}{\epsilon_d^2} \int_{-\infty}^{\infty} dy_4 \left[\text{th}\left(\frac{y_4 - \omega}{2T}\right) - \text{th}\frac{y_4}{2T} \right] \\ & \times \left[\rho(\mathbf{r}_{ij}, y_4 + \omega) \rho(\mathbf{r}_{ij}, -y_4 + \omega) G_c^{\text{R}}(\mathbf{r}_{ij}, -y_4) G_c^{\text{R}}(\mathbf{r}_{ij}, y_4) \right]. \end{aligned} \quad (14)$$

Therefore, to the leading order in ω and in the low temperature limit, $T \ll \epsilon_F$, $\text{Im}\Gamma^{\text{R}}(\omega + i\delta)/\omega$ is expressed in a compact form as

$$\frac{\text{Im}\Gamma_{\text{ph}}^{\text{R}}(\omega + i\delta)}{\omega} \approx \frac{4\pi V_{\text{dc}}^2 T U_{\text{ph}}}{\epsilon_d^2} \left[\rho(\mathbf{r}_{ij}, 0) G_c^{\text{R}}(\mathbf{r}_{ij}, 0) \right]^2. \quad (15)$$

With the use of definition Eq. (11) for the spectral function $\rho(\mathbf{r}, y)$, $\rho(\mathbf{r}, 0)$ is given by

$$\rho(\mathbf{r}, 0) = N_F \frac{e^{-(r/2\ell)}}{k_F r} \sin(k_F r), \quad (16)$$

and an explicit form of $G_c^{\text{R}}(\mathbf{r}, \epsilon)$ is given by

$$G_c^{\text{R}}(\mathbf{r}, \epsilon) = N_F \frac{e^{-(r/2\ell)}}{k_F r} \int_{-\epsilon_F}^{\epsilon_c} dy \sin \left[\sqrt{\frac{y}{\epsilon_F} + 1} (k_F r) \right] \frac{1}{\epsilon - y}. \quad (17)$$

Therefore, $G_c^{\text{R}}(\mathbf{r}, 0)$ is expressed as

$$G_c^{\text{R}}(\mathbf{r}, 0) = -N_F e^{-(r/2\ell)} J(k_F r), \quad (18)$$

with a function defined as

$$J(k_F r) \equiv \frac{1}{k_F r} \int_{-\epsilon_F}^{\epsilon_c} dy \sin \left[\sqrt{\frac{y}{\epsilon_F} + 1} (k_F r) \right] \frac{1}{y}. \quad (19)$$

The result of numerical integration in Eq. (19) is shown in Fig. 2 for a series of (ϵ_c/ϵ_F) s.

Substituting Eqs. (16) and (17) into Eq. (15), the NMR relaxation rate $(1/T_1 T)_{\text{ph}}$ [Eq. (7)] in the

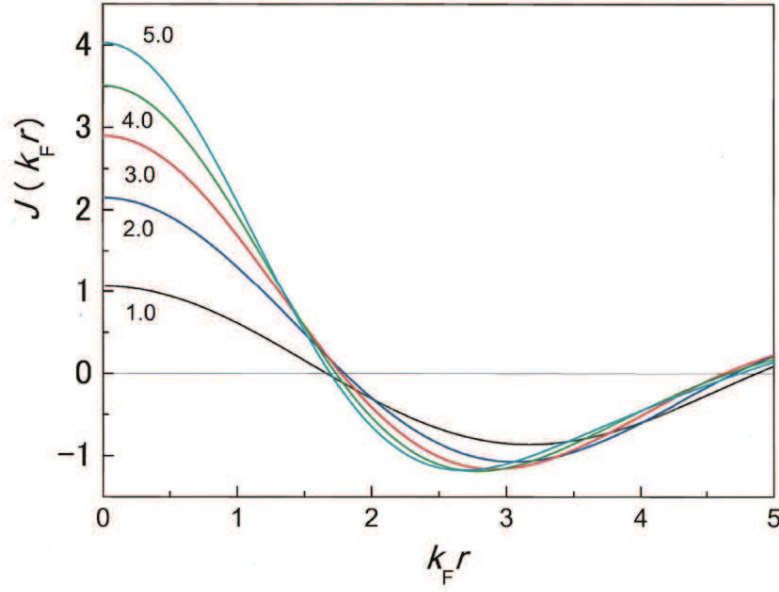


Fig. 2. $J(k_F r)$ for a series of (ϵ_c/ϵ_F) s.

low temperature limit ($T \ll \epsilon_F$) is given by

$$\left(\frac{1}{T_1 T}\right)_{\text{ph}} \approx A^2 \frac{4\pi N_F^2 (V_{\text{dc}} N_F)^2 T U_{\text{ph}}}{\epsilon_d^2} e^{-(r/\ell)} \left[\frac{\sin(k_F r)}{k_F r} J(k_F r) \right]^2. \quad (20)$$

This formula offers the basis for discussing anomalous enhancement of the relaxation rate $1/T_1 T$ in the region $T \gtrsim T_K$.

In the limit $k_F r \ll 1$, the integration with respect to y in Eq. (19) is given by

$$J(k_F r) \approx 2 \sqrt{\frac{\epsilon_F}{\epsilon_c} + 1} + \log \left| \frac{\sqrt{\epsilon_c + \epsilon_F} - \sqrt{\epsilon_F}}{\sqrt{\epsilon_c + \epsilon_F} + \sqrt{\epsilon_F}} \right|, \quad (21)$$

as shown in Appendix. On the other hand, in the limit $k_F r \gg 1$, the asymptotic form of $J(k_F r)$ is given as

$$J(k_F r) \approx \frac{1}{k_F r} \pi \cos(k_F r), \quad (22)$$

as shown in Appendix. Note that the asymptotic form shown in Fig. 2 is consistent with the result [Eq. (22)]. Therefore, in the limit $k_F r \gg 1$, $1/T_1 T$ given by Eq. (20) is in proportion to $e^{-(r/\ell)} [\sin(2k_F r)/(k_F r)^2]^2$.

According to the result based on the NRG calculation,⁵⁾ the renormalized pair-hopping interaction U_{ph} , owing to the impurity charge Kondo effect, is expected to exhibit a diverging T dependence as T decreases. This is because, as shown in Appendix, the U_{ph} is transformed to the spin exchange interaction by the particle-hole transformation for the down spin component of both localized (d) and conduction electrons, so that it is enhanced in parallel to the magnetic Kondo effect. Indeed, the

renormalization of U_{ph} up to the second order in U_{ph} and U_{dc} is given by the Feynman diagrams shown in Fig. 3(a). Similarly, that of U_{dc} is given by the Feynman diagram shown in Fig. 3(b). These processes are formally the same as those appearing the magnetic Kondo problem because U_{ph} and U_{dc} correspond to $J_{\perp}/2$ and $J_z/4$ in the anisotropic s-d model, respectively, in the mapped world by the transformations [Eqs. (A-1) and (A-2)] as discussed in Appendix.

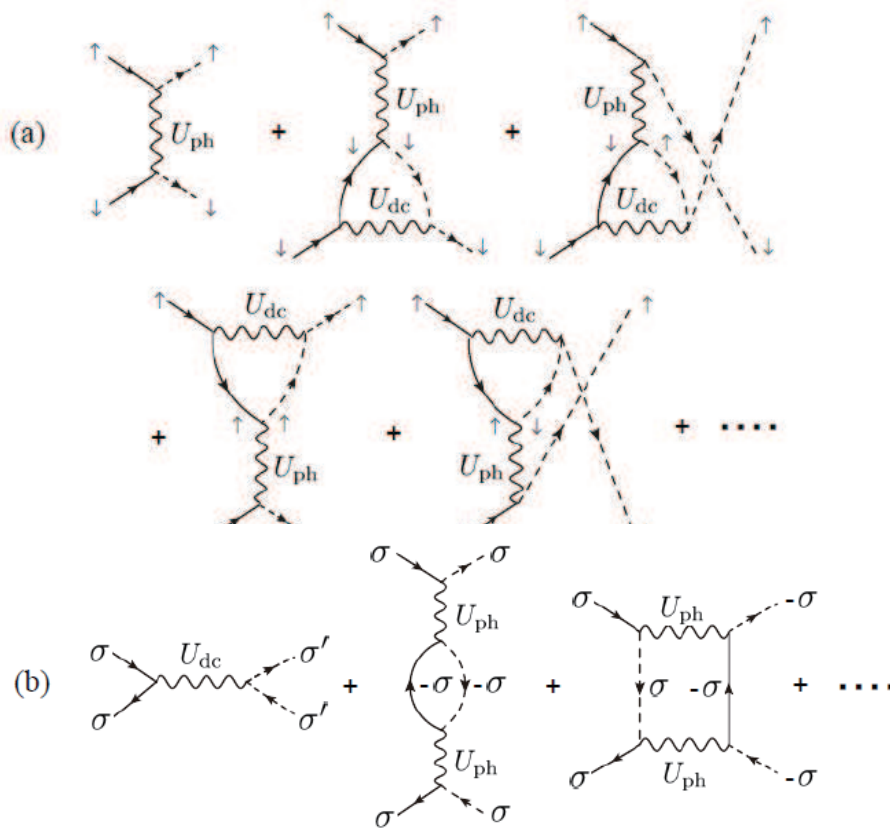


Fig. 3. Feynman diagram for the renormalization of (a) the pair-hopping interaction U_{ph} and (b) the inter-orbital interaction U_{dc} , up to the second order in U_{ph} and U_{dc} . These are formally the same as those in the anisotropic s-d model.

In order to take into account a series of higher order corrections with respect to U_{ph} and U_{dc} , it is useful to rely on RG approaches in general. For example, this type of approach has been successfully applied to understand the anomalous temperature dependence of the valence of the Sm ion in a filled-Skutterudite compound $\text{SmOs}_4\text{Sb}_{12}$.¹⁸⁾ Here, we adopt the one-loop order (or poorman' scaling) approximation.¹⁹⁾ As shown in Appendix [Eq. (G-8)], the T dependent renormalized pair-hopping interaction $U_{\text{ph}}(T) [\equiv y_{\perp}(T)/2N_{\text{F}}]$ is given as

$$U_{\text{ph}}(T) = \frac{1}{2N_{\text{F}} \log(T/T_{\text{K}})}, \quad (23)$$

and has the logarithmic T dependence, in the high temperature region at $T \gtrsim T_K$, like

$$U_{\text{ph}}(T) \approx U_{\text{ph}}^0 - 4N_{\text{F}}U_{\text{ph}}^0U_{\text{dc}}^0 \log \frac{T}{E_{\text{c}}^0}, \quad (24)$$

where U_{ph}^0 and U_{dc}^0 are the bare pair-hopping and inter-orbital interactions, respectively, and E_{c}^0 is the bare bandwidth of conduction electrons. On the other hand, $U_{\text{ph}}(T)$ exhibits divergent behavior toward $T = T_K$ as $U_{\text{ph}}(T) \approx U_{\text{ph}}^0 / \log(T/T_K)$ in the one-loop order RG approximation. Replacing U_{ph} in Eq. (20) by $U_{\text{ph}}(T)$ [Eq. (23)], the NMR relaxation rates $(1/T_1T)_{\text{ph}}$ at Te site (\mathbf{r}) is given by

$$\left(\frac{1}{T_1T} \right)_{\text{ph}} \approx A^2 \frac{4\pi N_{\text{F}}^2 (V_{\text{dc}} N_{\text{F}})^2}{\epsilon_{\text{d}}^2} e^{-(r/\ell)} \left[\frac{\sin(k_{\text{F}}r)}{k_{\text{F}}r} J(k_{\text{F}}r) \right]^2 T U_{\text{ph}}(T). \quad (25)$$

The procedure of replacing the bare pair-hopping interaction U_{ph}^0 by the renormalized one $U_{\text{ph}}(T)$ may be justified by the expression [Eq. (14)] in which major contribution comes from the conduction electrons with the energy $y_4 \lesssim T$. Equation (25) is one of central results of the present paper. Namely, the NMR relaxation rates $1/T_1T$ at Te sites near the Tl site should exhibit pronounced increase as T decreases toward the Kondo temperature T_K of the charge Kondo effect. This result is a signature of the diverging increase in the NMR relaxation rate $1/T_1T$ of ^{125}Te in $\text{Pb}_{1-x}\text{Tl}_x\text{Te}$ observed below $T = 10$ K for the sample $x \simeq 0.01$ in Ref. 13. Note that $1/T_1T$ of ^{125}Te in $\text{Pb}_{1-x}\text{Na}_x\text{Te}$ with non-valence skipping element Na does not exhibit such enhancement,²⁰⁾ suggesting that the valence skipping effect is the origin of such enhancement. The result is expected to remain essentially valid if we adopt more solid calculations, such as the NRG calculation,⁵⁾ because the diverging behavior in the renormalized pair-hopping interaction U_{ph} toward $T = T_K$ is still expected as discussed in the end of the present section.

Concluding this subsection, it should be remarked that there exist higher order corrections in U_{ph} to the diagram shown in Fig. 1 which is essentially independent of the Kondo-like renormalization on the pair-hopping interaction U_{ph} itself given by the vertical processes shown in Fig. 3(a). For example, such a next order correction $\Delta U_{\text{ph}}(i\omega_{\nu})$ to U_{ph} in Fig. 1 (in the horizontal direction) is given by Fig. 4 whose analytic expression is

$$\begin{aligned} \Delta U_{\text{ph}}(i\omega_{\nu}) &= -U_{\text{ph}}^2 T \sum_{\epsilon_{n''}} G_{\text{d}}(i\epsilon_{n''} + i\omega_{\nu}) G_{\text{d}}(-i\epsilon_{n''}) \\ &= -U_{\text{ph}}^2 \frac{1}{2\epsilon_{\text{d}} - i\omega_{\nu}} \tanh\left(\frac{\epsilon_{\text{d}}}{2T}\right), \end{aligned} \quad (26)$$

where the minus sign arises from the order of perturbation expansion with respect to U_{ph} compared to the first order term in U_{ph} given by Fig. 1. After analytic continuation $i\omega_{\nu} \rightarrow \omega + i\delta$, $\Delta U_{\text{ph}}^{\text{R}}(\omega + i\delta)$ is reduced to

$$\Delta U_{\text{ph}}^{\text{R}}(\omega + i\delta) = -U_{\text{ph}}^2 \frac{1}{2\epsilon_{\text{d}}} \tanh\left(\frac{\epsilon_{\text{d}}}{2T}\right), \quad (27)$$

where we have used the relation $\delta(\omega - \epsilon_d) = 0$ which holds at $\omega \sim 0$. This correction is negative and gives the suppression of the effect of the pair-hopping interaction in contrast to the enhancement by the Kondo-like renormalization given by the vertical processes shown in Fig. 3. This kind of counter renormalization effect is a general aspect of the Kondo effect in which the effect of the divergent increase of the effective exchange coupling constant J finally becomes inactive because of the Kondo-Yosida singlet formation^{25,26)} by the divergent exchange coupling constant itself.¹⁹⁾ Indeed, it was demonstrated that the vertex correction for the spin susceptibility is crucial to obtain the Korringa relation characteristic of the local Fermi liquid property in multi orbital d-electron impurity Anderson model.²⁸⁾ However, such an effect of renormalization becomes crucial only at $T < T_K$ where the Kondo-Yosida singlet state is formed. Therefore, it plays minor roles in the region $T \gtrsim T_K$ where the diverging T dependence in $1/T_1 T$ is observed.

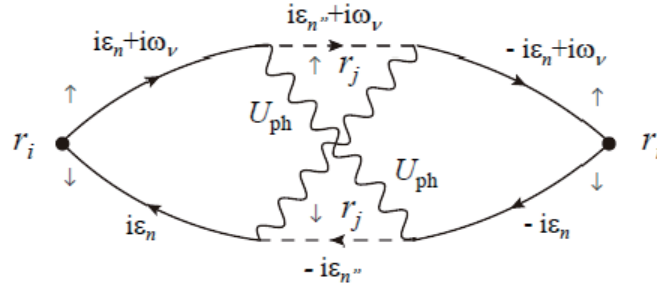


Fig. 4. Feynman diagram giving the NMR longitudinal relaxation rates $1/T_1 T$ at Te (\mathbf{r}_i) site in the second order in the pair-hopping interaction U_{ph} . Notations are the same as those of Fig. 1

3.2 Effect of inter-orbital interaction

In this subsection, the NMR relaxation rate triggered by the inter-orbital interaction U_{dc} . Although it was demonstrated that the pair-hopping interaction U_{ph} enhances the NMR relaxation rate toward $T = T_K$, it is crucial to note that the inter-orbital interaction U_{dc} is also renormalized (enhanced) by the charge Kondo effect, as shown in Appendix [Eq. (G-9)], and the T dependent $U_{dc}(T)$ also has the logarithmic T dependence in the high temperature region $T \gtrsim T_K$ as

$$U_{dc}(T) \approx U_{dc}^0 - N_F (U_{ph}^0)^2 \log \frac{T}{E_c^0}, \quad (28)$$

and exhibits divergent behavior toward $T = T_K$ as $U_{dc}(T) \approx 1/[4N_F \log(T/T_K)]$ in the one-loop order RG approximation, like in Eq. (23) as shown in Appendix . Therefore, we have to keep the relaxation processes caused by the effect of U_{dc} . There are three types of processes causing the relaxation in the first order in U_{dc} . One of them is given by the Feynman diagram shown in Fig. 5 or its vertical inver-

sion. This is a type of vertex correction to the local magnetic susceptibility of conduction electrons at certain Te site. Corresponding to the expression [Eq. (8)], the analytic expression for the function $\Gamma_{\text{dcV}}(i\omega_\nu)$ for this correction is given by

$$\Gamma_{\text{dcV}}(i\omega_\nu) = \frac{2V_{\text{dc}}^2}{\epsilon_{\text{d}}^2} T^2 \sum_{\epsilon_n} U_{\text{dc}} \left[G_{\text{c}}(\mathbf{r}_{ij}, i\epsilon_n) G_{\text{c}}(\mathbf{r}_{ij}, i\epsilon_n + i\omega_\nu) \right]^2, \quad (29)$$

where we have used the property $G_{\text{c}}(-\mathbf{r}_{ij}, i\epsilon_n) = G_{\text{c}}(\mathbf{r}_{ij}, i\epsilon_n)$ etc., and the factor 2 arises from the diagram of the inversion of upside down.

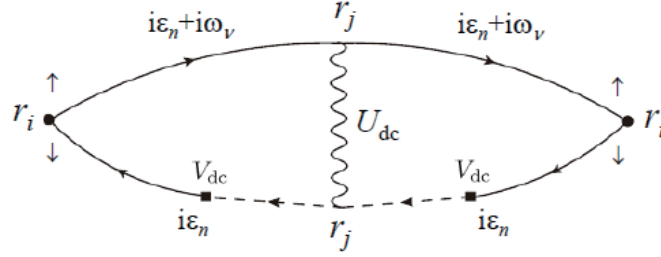


Fig. 5. Feynman diagram giving the NMR longitudinal relaxation rates $1/T_1T$ at Te (\mathbf{r}_i) site in the lowest order with respect to the inter-orbital interaction U_{dc} which corresponds to that given by Fig. 1. The other diagram is given by the inversion of upside down.

Other types of processes causing the relaxation are given by the Feynman diagrams shown in Figs. 6(a) and (b) and Figs. 7(a) and (b). These are a type of the self-energy corrections to the conduction electrons. It is easy to see that the contribution from Figs. 7(a) and (b) is twice of that from Figs. 6(a) and (b), due to spin degrees of freedom, with negative sign due to the extra Fermion-loop factor (-1) . Therefore, the analytic expression for the function $\Gamma_{\text{dcS}}(i\omega_\nu)$ corresponding to diagrams shown in Figs. 6(a) and (b) and Figs. 7(a) and (b) is given as

$$\Gamma_{\text{dcS}}(i\omega_\nu) = -\frac{2V_{\text{dc}}^2}{\epsilon_{\text{d}}^2} T^2 \sum_{\epsilon_n} U_{\text{dc}} \left\{ [G_{\text{c}}(\mathbf{r}_{ij}, i\epsilon_n)]^2 G_{\text{c}}(0, i\epsilon_n) G_{\text{c}}(0, i\epsilon_n - i\omega_\nu) [G_{\text{d}}(i\epsilon_n)]^2 \right. \\ \left. + [G_{\text{c}}(\mathbf{r}_{ij}, i\epsilon_n)]^2 G_{\text{c}}(0, i\epsilon_n) G_{\text{c}}(0, i\epsilon_n + i\omega_\nu) [G_{\text{d}}(i\epsilon_n)]^2 \right\}, \quad (30)$$

where the first and second terms are for the Figs. 6(a) and (b), respectively, and the factor 2 arises from the diagram of the inversion of upside down.

Performing calculations similar to that obtaining the expression Eq. (14) for $\text{Im}\Gamma_{\text{ph}}^{\text{R}}(\omega + i\delta)$, the expression of $\text{Im}\Gamma_{\text{dcV}}^{\text{R}}(\omega + i\delta)$ is given, to the leading order in ω , as

$$\text{Im}\Gamma_{\text{dcV}}^{\text{R}}(\omega + i\delta) = -\frac{4\pi\omega V_{\text{dc}}^2 T U_{\text{dc}}}{\epsilon_{\text{d}}^2} \int_{-\infty}^{\infty} dy \frac{\partial}{\partial y} \left(\text{th} \frac{y}{2T} \right) \left[\rho(\mathbf{r}_{ij}, y) G_{\text{c}}^{\text{R}}(\mathbf{r}_{ij}, y) \right]^2. \quad (31)$$

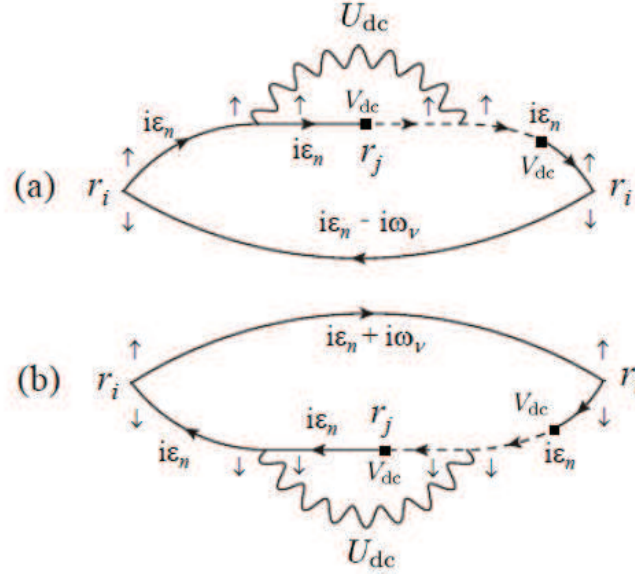


Fig. 6. Feynman diagram giving the NMR longitudinal relaxation rates $1/T_1T$ at Te (\mathbf{r}_i) site in the lowest order with respect to the inter-orbital interaction U_{dc} which corresponds to a Fock type self-energy correction. The other diagrams are given by the mirror inversion with respect to U_{dc} .

Then, in the low temperature limit ($T \ll \epsilon_F$), the $\text{Im}\Gamma_{dcV}^R(\omega + i\delta)/\omega$ is reduced to a compact form as

$$\frac{\text{Im}\Gamma_{dcV}^R(\omega + i\delta)}{\omega} \approx -\frac{8\pi V_{dc}^2 T U_{dc}}{\epsilon_d^2} [\rho(\mathbf{r}_{ij}, 0) G_c'^R(\mathbf{r}_{ij}, 0)]^2. \quad (32)$$

This term has the same form as Eq. (15) giving $\text{Im}\Gamma_{ph}^R(\omega + i\delta)/\omega$ with U_{ph} being replaced by $-U_{dc}$. Therefore, it has an effect that U_{ph} in Eq. (15) is replaced by $(U_{ph} - 2U_{dc})$.

Similarly, the expression of $\text{Im}\Gamma_{dcS}^R(\omega + i\delta)$ is given, to the leading order in ω , as

$$\text{Im}\Gamma_{dcS}^R(\omega + i\delta) = \frac{6\pi\omega V_{dc}^2 T U_{dc}}{\epsilon_d^2} \int_{-\infty}^{\infty} dy_3 \frac{\partial}{\partial y_3} \left(\text{th} \frac{y_3}{2T} \right) [\rho(0, y_3) G_c'^R(\mathbf{r}_{ij}, y_3)]^2. \quad (33)$$

Then, in the low temperature limit ($T \ll \epsilon_F$), the $\text{Im}\Gamma_{dcS}^R(\omega + i\delta)/\omega$ [Eq. (33)] is reduced to a compact form as

$$\frac{\text{Im}\Gamma_{dcS}^R(\omega + i\delta)}{\omega} \approx \frac{12\pi V_{dc}^2 T U_{dc}}{\epsilon_d^2} [\rho(0, 0) G_c'^R(\mathbf{r}_{ij}, 0)]^2. \quad (34)$$

Substituting the expressions for $\rho(0, 0)$ [Eq. (16)] and $G_c'^R(\mathbf{r}_{ij}, 0)$ [Eq. (18)] and replacing the bare inter-orbital interaction U_{dc}^0 by the renormalized one, $U_{dc}(T)$ [Eq. (G-9)], the relaxation rate $(1/T_1T)_{dcS}$ [Eq. (7)] is given as

$$\left(\frac{1}{T_1T} \right)_{dcS} \approx A^2 \frac{12\pi(V_{dc} N_F)^2}{\epsilon_d^2} e^{-(r/\ell)} \left[\frac{\sin(k_F r)}{k_F r} J(k_F r) \right]^2 T U_{dc}(T). \quad (35)$$

This formula is another central results of the present paper and offers us the basis for discussing anomalous behavior of the relaxation rate $1/T_1T$ in the region $T \sim T_K$.

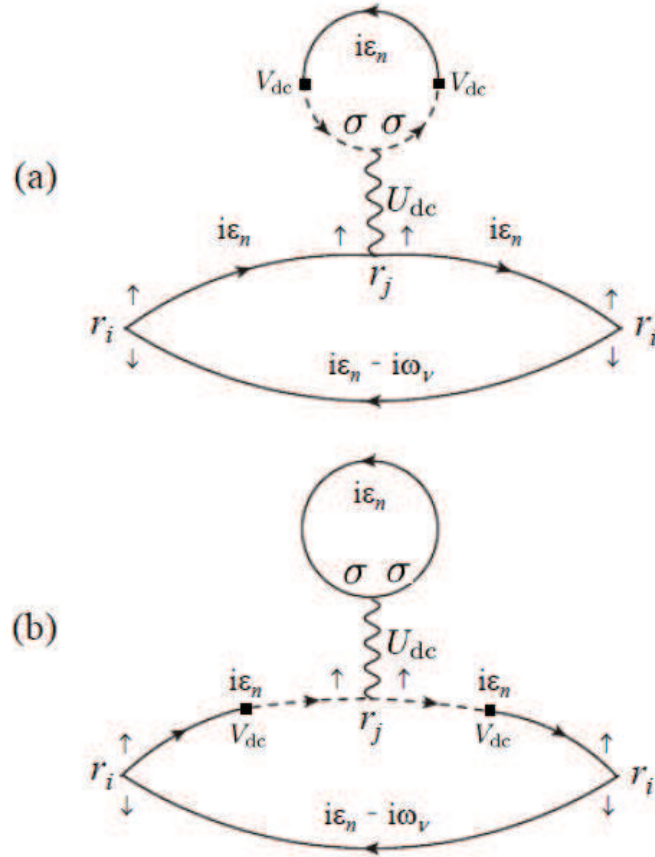


Fig. 7. Feynman diagram giving the NMR longitudinal relaxation rates $1/T_1T$ at Te (r_i) site in the lowest order with respect to the inter-orbital interaction U_{dc} which corresponds to a Hartree type self-energy correction. The summation with respect to spin component $\sigma = \uparrow$ and \downarrow . The other diagrams are given by the inversion of upside down.

3.3 Short summary for NMR relaxation rate

The total relaxation rate $(1/T_1T)$ is given by the sum of $(1/T_1T)_{ph}$ [Eq. (25)], $(1/T_1T)_{dcv}$ [Eq. (32)], and $(1/T_1T)_{dcs}$ [Eq. 35)] as follows:

$$\begin{aligned} \frac{1}{T_1T} \approx & A^2 \frac{4\pi N_F^2 (V_{dc} N_F)^2}{\epsilon_d^2} e^{-(r/\ell)} \left[\frac{\sin(k_F r)}{k_F r} J(k_F r) \right]^2 T [U_{ph}(T) - 2U_{dc}(T)] \\ & + A^2 \frac{12\pi N_F^2 (V_{dc} N_F)^2}{\epsilon_d^2} e^{-(r/\ell)} \left[\frac{\sin(k_F r)}{k_F r} J(k_F r) \right]^2 T U_{dc}(T), \end{aligned} \quad (36)$$

where we have used the expressions of $U_{ph}(T)$ [Eq. (G-8)] and $U_{dc}(T)$ [Eq. (G-9)]. Since U_{ph} and U_{dc} correspond to $J_{\perp}/2$ and $J_z/4$, respectively, as discussed in Appendices and , the ratio of $[U_{ph}(T) - 2U_{dc}(T)]$ in the first term of Eq. (36) and $U_{ph}(T)$ approaches zero toward $T = T_K$ as decreasing

temperature. Therefore, the first term gives less divergent behavior compared to the second term. On the other hand, the second term in Eq. (36) exhibits pronounced increase as T decreases, toward $T = T_K$ from the region $T \gtrsim T_K$, through the T dependence of $TU_{dc}(T)$ (in a dimensionless form) shown in Fig. 8 in which the T dependence of $U_{dc}(T)$ is given by the one-loop order RG (or poorman's scaling) approximation as

$$U_{dc}(T) = \frac{1}{4N_F \log \frac{T}{T_K}}. \quad (37)$$

(See Eq. (G-10) for y_z and definition of $U_{dc}(E) \equiv y_z/4N_F$ in Appendix .) Of course, the result of poorman's scaling ceases to be valid very near $T = T_K$. Nevertheless, it would give an increasing tendency of $TU_{dc}(T)$ around $T = T_K$. The dotted line in Fig. 8 shows an expected T dependence of $TU_{dc}(T)$ at $T \lesssim T_K$, which is reasonable considering that the increasing tendency of $TU_{dc}(T)$ already begins to appear at $T \simeq 2.7T_K$, i.e., from far higher temperature than T_K , and that the divergent T dependence in $U_{dc}(T)$ at $T \ll T_K$ works to suppress the Curie like divergence ($\propto 1/T$) of localized electron when entering into the local Fermi liquid state²⁷⁾ in which the Kondo-Yosida charge singlet state is formed as in the case of magnetic Kondo problem.²⁸⁾ Since the *divergent* part in $1/T_1T$ [Eq. (36)] is in proportion to $TU_{dc}(T)$, this theoretical result for $1/T_1T$ qualitatively explains the anomalous temperature dependence of $1/T_1T$ observed in $\text{Pb}_{1-x}\text{Tl}_x\text{Te}$ ($x \simeq 0.01$) reported in Ref. 13. However, of course to obtain more quantitative result for the T dependence in $1/T_1T$ at $T \lesssim T_K$, we need perform more solid calculations, such as numerical renormalization group method,⁵⁾ which is left for future study.

Concluding this section, it is remarked that the present relaxation mechanism is quite different from the case of magnetic Kondo impurity in which $1/T_1T$ is essentially in proportion to J_\perp^2 as discussed in Ref. 21. This difference is traced back to the difference in the order of perturbation process giving the relaxation rates. In the present case, $1/T_1T$ is given by the first order process in the pair-hopping interaction U_{ph} and the inter-orbital interaction U_{dc} , while that in the case of magnetic Kondo impurity is given by the second order process in the s-d exchange interaction J_\perp causing the spin-flip process, as discussed in Ref. 21

4. Anomaly of Knight Shift by Charge Kondo Effect

The temperature dependence of the Knight shift K is related with $(1/T_1T)$ through the Kramers-Kronig relation among the real and the imaginary part of the *local* dynamical magnetic susceptibility $\chi(\omega + i\delta)$ at the site of the NMR measurement. This is because the Knight shift K is proportional to the real part of $\chi(0)$ while $(1/T_1T)$ is given by the imaginary part of $\chi(\omega + i\delta)/\omega$ by the Moriya formula

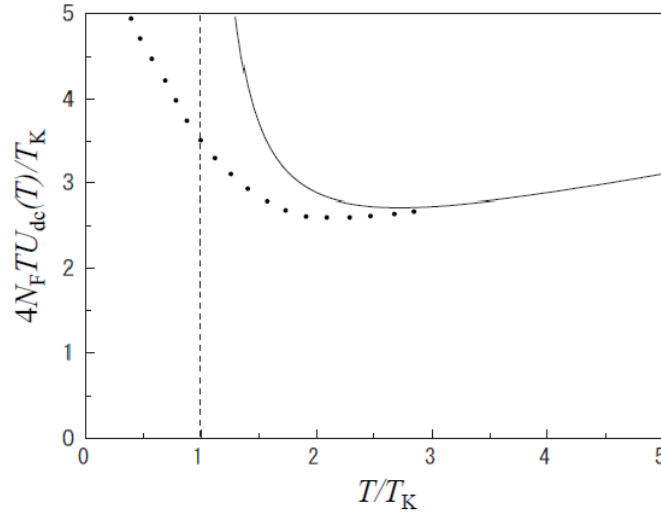


Fig. 8. $4N_F T U_{dc}(T)/T_K$ vs T/T_K with T_K being the Kondo temperature in the one-loop order RG (poorman's scaling) approximation [Eq. (D·2)]. Dotted line is a guide to the eyes for a qualitative behavior expected in exact treatment beyond poorman's scaling solution as discussed in the text.

[Eq. (7)] as

$$\begin{aligned} \frac{1}{T_1 T} &= A^2 \left[\frac{1}{\omega} \text{Im} \chi(\omega + i\delta) \right]_{\omega=\omega_{\text{NMR}}} \\ &\simeq A^2 \left[\frac{1}{\omega} \text{Im} \chi(\omega + i\delta) \right]_{\omega=0}, \end{aligned} \quad (38)$$

where A is the hyper-fine coupling constant between electrons (quasiparticles) and nuclei,¹⁴⁾ and ω_{NMR} is the frequency of NMR measurement. The explicit form of the Kramers-Kronig relation for $\chi(\omega + i\delta) \equiv \chi'(\omega) + i\chi''(\omega)$ is

$$\chi'(\omega) = \frac{1}{\pi} \mathcal{P} \int_{-\infty}^{\infty} d\omega' \frac{\chi''(\omega')}{\omega' - \omega}. \quad (39)$$

Therefore, the real part of $\chi'(0)$ is given by the imaginary part of $\chi''(\omega)$ as

$$\chi'(0) = \frac{1}{\pi} \int_{-\infty}^{\infty} d\omega' \frac{\chi''(\omega')}{\omega'}. \quad (40)$$

Here, we adopt the following parameterization:

$$\chi''(\omega) = \omega \left[\lim_{\omega \rightarrow 0} \frac{\chi''(\omega)}{\omega} \right] R(\omega). \quad (41)$$

Note that the second factor $\lim_{\omega \rightarrow 0} [\chi''(\omega)/\omega]$, or $(1/T_1 T)$, exhibits increasing tendency as the temperature decreases across the Kondo temperature T_K as discussed in subsection 3.3. On the other hand, the remnant factor $R(\omega)$ is a positive, even and decreasing function in ω , with $\lim_{\omega \rightarrow 0} R(\omega) = 1$ and $\lim_{|\omega| \rightarrow \infty} R(\omega) \propto \omega^{-2}$ at least.³¹⁾ Otherwise, it exhibits a moderate ω - and T -dependence in entire ω

region. As a result, the correction to the Knight shift ΔK , given with the use of $\Delta\chi'(0)$ [cf. Eq. (40)], exhibits the anomaly similar to the correction to the NMR relaxation rate $\Delta(1/T_1T)$. This is because the following relation holds.

$$\Delta K = A\Delta\chi'(0) \simeq \Delta\left(\frac{1}{T_1T}\right) \frac{1}{\pi A} \int_{-\infty}^{\infty} d\omega' R(\omega'), \quad (42)$$

where the integration of $R(\omega')$ is expected to have only weak T -dependence, because the most dominant T -dependence in $\chi''(\omega)$ has been taken into account by the second factor in Eq. (41).

Indeed, such T increasing tendency of the Knight shift around T_K has been recently observed by experiment.³²⁾ This implies that the Korringa relation $1/T_1T \propto K^2$ is apparently broken in general. Here, it is crucial that the present subject is the *local* impurity problem which is free from the long range magnetic correlations due to, e.g., the enhanced antiferromagnetic fluctuations as observed in the case of high T_c cuprates.³³⁾

The aspect of the Knight shift discussed here has been verified by explicit microscopic calculations similar to obtaining the anomalous behavior of the NMR relaxation rate $1/T_1$, which will be published elsewhere.

5. Summary

We have shown that the anomalous NMR response observed in $\text{Pb}_{1-x}\text{Tl}_x\text{Te}$ ($x \sim 0.01$) can be explained by the charge Kondo effect which is caused by the pair-hopping interaction U_{ph} and the inter-orbital interaction U_{dc} between localized orbital on Tl and conduction electrons doped in the semiconductor PbTe. Sharp increase observed in the NMR relaxation rate $1/T_1T$ of ^{125}Te at $T < 10\text{K}$ can be understood essentially as the increase of U_{ph} and U_{dc} due to Kondo-like renormalization in the region $T \gtrsim T_K$ because U_{ph} and U_{dc} can mediate the spin-flip of conduction electrons as shown in Fig. 1, and Figs. 5, 6, and 7, respectively. We have also shown that the Knight shift K is also enhanced in proportion to the relaxation rate $1/T_1T$ in the region of temperature where $1/T_1T$ is enhanced. In this sense, the Korringa relation is apparently broken in the system with the charge Kondo effect.

Acknowledgments

We are grateful to H. Mukuda for stimulating discussions on the experimental results of ^{125}Te NMR in $\text{Pb}_{1-x}\text{Tl}_x\text{Te}$ ($x=0.01$). This work is supported by the Grant-in-Aid for Scientific Research (Nos. 15K17694 and 17K05555) from the Japan Society for the Promotion of Science.

Appendix A: Equivalence of Pair-Hopping and Inter-orbital Interactions to Pseudo-Spin Exchange Interactions

Here we discuss why the pair-hopping interaction U_{ph} is enhanced in the scattering channel $i\varepsilon_n \rightarrow -i\varepsilon_n$, shown in Figs. A·1 and D·1. The reason why it is enhanced by the charge Kondo effect is understood intuitively by the fact that the pair-hopping interaction is mapped to that of spin-flipping interaction, i.e., the heart of the Kondo interaction, by the canonical transformation for both the localized electron d and conduction electrons with \downarrow spin and \uparrow spin as

$$d_{\downarrow}^{\dagger} \rightarrow \tilde{d}_{\downarrow} \quad \text{and} \quad c_{\mathbf{k}\downarrow}^{\dagger} \rightarrow \tilde{c}_{\mathbf{k}\downarrow}, \quad (\text{A}\cdot 1)$$

$$d_{\uparrow}^{\dagger} \rightarrow \tilde{d}_{\uparrow}^{\dagger} \quad \text{and} \quad c_{\mathbf{k}\uparrow}^{\dagger} \rightarrow \tilde{c}_{\mathbf{k}\uparrow}^{\dagger}. \quad (\text{A}\cdot 2)$$

This is a variant of the canonical transformation introduced by Shiba.^{22,23)} Namely, by the transformations [Eqs. (A·1) and (A·2)], the pair-hopping interaction is mapped as follows:

$$\begin{aligned} U_{\text{ph}} \sum_{\mathbf{k}, \mathbf{k}'} \left(d_{\uparrow}^{\dagger} d_{\downarrow}^{\dagger} c_{\mathbf{k}\downarrow} c_{\mathbf{k}'\uparrow} + \text{h.c.} \right) \\ \rightarrow U_{\text{ph}} \sum_{\mathbf{k}, \mathbf{k}'} \left(\tilde{d}_{\uparrow}^{\dagger} \tilde{d}_{\downarrow} \tilde{c}_{\mathbf{k}\downarrow}^{\dagger} \tilde{c}_{\mathbf{k}'\uparrow} + \text{h.c.} \right) \equiv U_{\text{ph}} \left(\tilde{S}_{\text{d}}^{+} \tilde{S}_{\mathbf{k}, \mathbf{k}'}^{-} + \text{h.c.} \right). \end{aligned} \quad (\text{A}\cdot 3)$$

Therefore, the pair-hopping interaction U_{ph} , which is equivalent to $J_{\perp}/2$ in the anisotropic s-d model¹⁹⁾ is enhanced by the Kondo effect in the mapped world. The spin-flipping exchange interaction U_{ph} in the mapped world is represented by the Feynman diagram shown in Fig. A·1(a), while the pair-hopping interaction U_{ph} in the original world is given by the Feynman diagram shown in Fig. A·1(b). Note that the Matsubara frequency of the conduction electrons with \downarrow spin has the opposite sign of that of the \uparrow spin because the direction of propagation in the imaginary time is opposite. Namely, the elastic scattering with $i\varepsilon_n \rightarrow i\varepsilon_n$ in the mapped world causing the Kondo effect corresponds to the scattering with $i\varepsilon_n \rightarrow -i\varepsilon_n$ in the original world. This is the reason why the process shown in Fig. 1 is selectively enhanced.

By the transformation [Eqs. (A·1) and (A·2)], the spin dependent density of states (DOS), $D_{\sigma}(\varepsilon)$, of conduction electrons and localized d electron change from that shown in Fig. A·2(a) to that in Fig. A·2(b). Namely, symmetry with respect to \uparrow and \downarrow spins is broken. Nevertheless, the Kondo effect is possible if the finite DOS of conduction electrons remain at the Fermi level and the energy level of localized electron with \uparrow and \downarrow spins are degenerate, i.e., $\varepsilon_{\text{d}} = -\varepsilon_{\text{d}} - U_{\text{dc}}$, as shown in Fig. A·2. The latter condition is satisfied in the negative- U Anderson model for rather wide doping rates of negative- U ions as discussed in ref. 4. It was also shown by the present authors⁵⁾ that the negative- U effect is realized in the model described by the Hamiltonian [Eq. (1)]. In this sense, it is assured that the condition for zero magnetic field on the localized electron is satisfied in a self-consistent fashion.

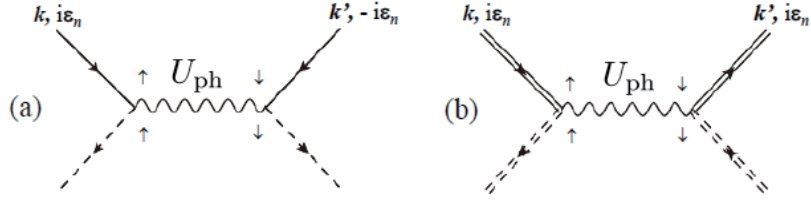


Fig. A-1. (a) Feynman diagram representing the pair-hopping process in the original world, and (b) Feynman diagram representing the spin-flipping exchange process in the mapped world by the canonical transformation [Eqs. (A-1) and (A-2)]. Wavy line represents the pair-hopping interaction U_{ph} , lines with arrow represent the Green function of conduction electrons in the original world, and double lines represent that in the mapped world. Dashed lines with arrow denote the Green functions of the localized electron d both in original and mapped worlds.

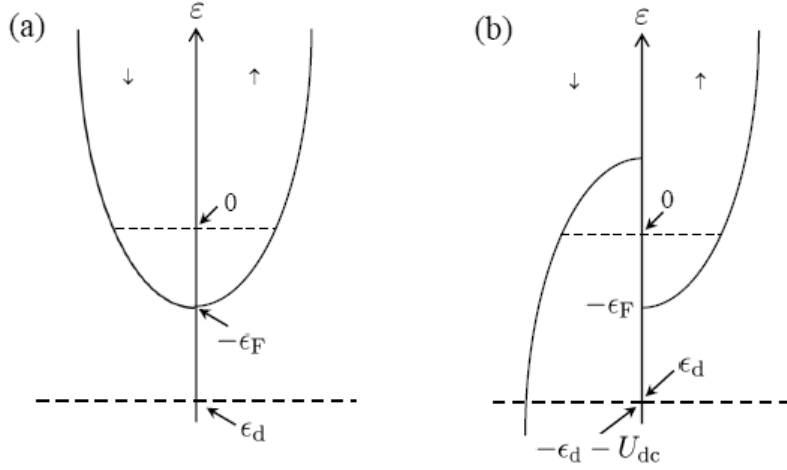


Fig. A-2. Spin dependent DOS, $D_\sigma(\varepsilon)$: (a) in the original world, and (b) in the transformed world by the transformation Eqs. Eqs. (A-1) and (A-2). Note that the origin of energy is ε_F , or energy is measured from ε_F .

Similarly, the inter-orbital interaction U_{dc} is also enhanced by the charge Kondo effect. Indeed, the inter-orbital interaction is mapped by the transformations [Eqs. (A-1) and (A-2)] as follows:

$$\begin{aligned}
 U_{dc} \sum_{\mathbf{k}, \mathbf{k}'} \sum_{\sigma \sigma'} d_\sigma^\dagger d_\sigma c_{\mathbf{k}\sigma'} c_{\mathbf{k}'\sigma'} \\
 \rightarrow U_{dc} \sum_{\mathbf{k}, \mathbf{k}'} (\tilde{d}_\uparrow^\dagger \tilde{d}_\uparrow - \tilde{d}_\downarrow^\dagger \tilde{d}_\downarrow) (\tilde{c}_{\mathbf{k}\uparrow}^\dagger \tilde{c}_{\mathbf{k}'\uparrow} - \tilde{c}_{\mathbf{k}\downarrow}^\dagger \tilde{c}_{\mathbf{k}'\downarrow}) \equiv 4U_{dc} \tilde{S}_d^z \tilde{S}_{\mathbf{k}, \mathbf{k}'}^z. \quad (\text{A-4})
 \end{aligned}$$

Therefore, the inter-orbital interaction U_{dc} is enhanced by the Kondo effect in the mapped world because it corresponds to $J_z/4$ in the anisotropic s-d model.⁶⁾ In this sense, the pair-hopping interaction U_{ph} and inter-orbital interaction U_{dc} should be treated impartially as in the case of magnetic Kondo

effect.⁶⁾

Appendix B: Spectral Function of Conduction Electrons

In this Appendix, we derive the spectral function, Eq. (11), for the conduction electrons. First, we note that the Green function $G_c(\mathbf{r}, i\varepsilon_n)$ of conduction electrons with impurity scattering is given by

$$G_c(\mathbf{r}, i\varepsilon_n) = e^{-(r/2\ell)} G_c^{(0)}(\mathbf{r}, i\varepsilon_n), \quad (\text{B}\cdot 1)$$

where ℓ is the mean-free path of the impurity scattering, and $G_c^{(0)}(\mathbf{r}, i\varepsilon_n)$ is the Green function in the pure system without impurity scattering.²⁴⁾ An explicit form of $G_c^{(0)}(\mathbf{r}, i\varepsilon_n)$ is calculated as follows:

$$\begin{aligned} G_c^{(0)}(\mathbf{r}, i\varepsilon_n) &= \frac{1}{N} \int \frac{d\mathbf{k}}{(2\pi)^3} \frac{e^{i\mathbf{k}\cdot\mathbf{r}}}{i\varepsilon_n - \xi_k} \\ &= \frac{1}{2\pi^2 N} \frac{1}{r} \int_0^{k_c} dk k \sin(kr) \frac{1}{i\varepsilon_n - \xi_k}, \end{aligned} \quad (\text{B}\cdot 2)$$

where the system volume is taken as the unit of volume, N is the number of lattice sites, and $\xi_k \equiv (k^2/2m) - \mu$, and we have introduced the upper cut-off wave number k_c . Then, the imaginary part of the retarded function $\text{Im}G_c^{(0)\text{R}}(\mathbf{r}, \varepsilon + i\delta)$ is calculated as follows:

$$\begin{aligned} \text{Im}G_c^{(0)\text{R}}(\mathbf{r}, \varepsilon + i\delta) &= -\frac{1}{2\pi N} \frac{1}{r} \int_0^{k_c} dk k \sin(kr) \delta(\varepsilon - \xi_k) \\ &= -\frac{m}{2\pi N} \frac{1}{r} \int_{-\varepsilon_F}^{\varepsilon_c} d\xi \sin \left[\sqrt{\frac{2m\xi}{k_F^2} + 1} (k_F r) \right] \delta(\varepsilon - \xi) \\ &= -\frac{m}{2\pi N} \frac{1}{r} \sin \left[\sqrt{\frac{\varepsilon}{\varepsilon_F} + 1} (k_F r) \right] \theta(\varepsilon + \varepsilon_F) \theta(\varepsilon - \varepsilon_c), \end{aligned} \quad (\text{B}\cdot 3)$$

where we have approximated μ by $-\varepsilon_F$ because we are interested in the low temperature region $T \ll \varepsilon_F$ and ε_c is the upper cut-off energy corresponding to k_c . Therefore, the spectral function $\rho(\mathbf{r}, \varepsilon) \equiv -(1/\pi) \text{Im}G_c^{(0)\text{R}}(\mathbf{r}, \varepsilon + i\delta)$ is given by Eq. (11).

Appendix C: Calculation of $\Gamma_{\text{ph}}^{\text{R}}(\omega + i\delta)$

In this Appendix, we calculate the expression [Eq. (8)] and derive the expression of $\text{Im}\Gamma_{\text{ph}}^{\text{R}}$ [Eq. (14)]. As is justified in Appendix, $G_d(-i\varepsilon_n + i\omega_\nu)G_d(i\varepsilon_n)$ in Eq. (8) can be approximated by $1/\varepsilon_d^2$. Then, $\tilde{\Gamma}_{\text{ph}}(i\omega_\nu) \equiv \Gamma_{\text{ph}}(i\omega_\nu)/T$ [see Eq. (8)] is given as

$$\tilde{\Gamma}_{\text{ph}}(i\omega_\nu) = \frac{2V_{\text{dc}}^2 U_{\text{ph}}}{\varepsilon_d^2} T \sum_{\varepsilon_n} \left(\prod_{\ell=1}^4 \int_{-\infty}^{\infty} dy_\ell \right) \frac{\rho(\mathbf{r}_{ij}, y_1)}{i\varepsilon_n - y_1} \frac{\rho(\mathbf{r}_{ij}, y_2)}{i\varepsilon_n + i\omega_\nu - y_2} \frac{\rho(\mathbf{r}_{ij}, y_3)}{-i\varepsilon_n - y_3} \frac{\rho(\mathbf{r}_{ij}, y_4)}{-i\varepsilon_n + i\omega_\nu - y_4}. \quad (\text{C}\cdot 1)$$

The summation with respect to ε_n is performed in a standard way by transforming the summation to the integration along the axes $\text{Im}z = 0$ and $\text{Im}z = \pm\omega_\nu$ on z -plane, where one is just above these axes

and another is just below in the counter direction. The result along $\text{Im}z = 0$, $\Gamma_1(i\omega_v)$, is given by

$$\Gamma_1(i\omega_v) = \frac{2V_{\text{dc}}^2 U_{\text{ph}}}{\epsilon_{\text{d}}^2} \left(\prod_{\ell=1}^4 \int_{-\infty}^{\infty} dy_{\ell} \right) \rho(\mathbf{r}_{ij}, y_1) \rho(\mathbf{r}_{ij}, y_2) \rho(\mathbf{r}_{ij}, y_3) \rho(\mathbf{r}_{ij}, y_4) \\ \times \text{th} \left(\frac{y_1}{2T} \right) \frac{1}{y_1 + y_3} \frac{1}{y_1 - y_2 + i\omega_v} \frac{1}{-y_1 - y_4 + i\omega_v}, \quad (\text{C-2})$$

and those along $\text{Im}z = \pm\omega_v$, $\Gamma_{\text{II}}(i\omega_v)$, are both given by

$$\Gamma_{\text{II}}(i\omega_v) = -\frac{V_{\text{dc}}^2 U_{\text{ph}}}{\epsilon_{\text{d}}^2} \left(\prod_{\ell=1}^4 \int_{-\infty}^{\infty} dy_{\ell} \right) \rho(\mathbf{r}_{ij}, y_1) \rho(\mathbf{r}_{ij}, y_2) \rho(\mathbf{r}_{ij}, y_3) \rho(\mathbf{r}_{ij}, y_4) \\ \times \text{th} \left(\frac{y_2}{2T} \right) \frac{1}{y_2 - y_1 - i\omega_v} \frac{1}{-y_2 - y_3 + i\omega_v} \frac{1}{-y_2 - y_4 + 2i\omega_v}. \quad (\text{C-3})$$

After analytic continuation, $i\omega_v \rightarrow \omega + i\delta$ in Eq. (C-2), and taking an imaginary part, we obtain

$$\text{Im}\Gamma_1^{\text{R}}(\omega + i\delta) = \frac{2\pi V_{\text{dc}}^2 U_{\text{ph}}}{\epsilon_{\text{d}}^2} \left(\prod_{\ell=1}^4 \int_{-\infty}^{\infty} dy_{\ell} \right) \rho(\mathbf{r}_{ij}, y_1) \rho(\mathbf{r}_{ij}, y_2) \rho(\mathbf{r}_{ij}, y_3) \rho(\mathbf{r}_{ij}, y_4) \\ \times \text{th} \left(\frac{y_4 - \omega}{2T} \right) \frac{1}{y_2 + y_4 - 2\omega} \left[\frac{\delta(y_1 + y_4 - \omega)}{-y_3 + y_4 - \omega} + \frac{\delta(y_1 - y_4 + \omega)}{y_3 + y_4 - \omega} \right], \quad (\text{C-4})$$

where and hereafter the integration implies the principal value integration. In deriving E. (C-4), we have used the property that $\rho(\mathbf{r}_{ij}, y_2)\rho(\mathbf{r}_{ij}, y_4)$ is symmetric with respect to interchange $y_2 \rightleftharpoons y_4$. Similarly, for Eq. (C-3), we obtain

$$\text{Im}\Gamma_{\text{II}}^{\text{R}}(\omega + i\delta) = -\frac{\pi V_{\text{dc}}^2 U_{\text{ph}}}{\epsilon_{\text{d}}^2} \left(\prod_{\ell=1}^4 \int_{-\infty}^{\infty} dy_{\ell} \right) \rho(\mathbf{r}_{ij}, y_1) \rho(\mathbf{r}_{ij}, y_2) \rho(\mathbf{r}_{ij}, y_3) \rho(\mathbf{r}_{ij}, y_4) \\ \times \text{th} \left(\frac{y_2}{2T} \right) \left\{ \frac{1}{y_2 + y_4 - 2\omega} \left[\frac{\delta(y_2 - y_1 - \omega)}{y_2 + y_3 - \omega} - \frac{\delta(y_2 + y_3 - \omega)}{y_1 - y_2 + \omega} \right] \right. \\ \left. - \frac{\delta(y_2 + y_4 - 2\omega)}{(y_1 - y_2 + \omega)(y_2 + y_3 - \omega)} \right\}. \quad (\text{C-5})$$

Performing the integration with respect to y_1 , Eq. (C-4) is reduced to

$$\text{Im}\Gamma_1^{\text{R}}(\omega + i\delta) = \frac{2\pi V_{\text{dc}}^2 U_{\text{ph}}}{\epsilon_{\text{d}}^2} \left(\prod_{\ell=2}^4 \int_{-\infty}^{\infty} dy_{\ell} \right) \text{th} \left(\frac{y_4 - \omega}{2T} \right) \frac{\rho(\mathbf{r}_{ij}, y_2) \rho(\mathbf{r}_{ij}, y_3) \rho(\mathbf{r}_{ij}, y_4)}{y_2 + y_4 - 2\omega} \\ \times \left[\frac{\rho(\mathbf{r}_{ij}, y_4 - \omega)}{y_3 + y_4 - \omega} - \frac{\rho(\mathbf{r}_{ij}, \omega - y_4)}{y_3 - y_4 + \omega} \right]. \quad (\text{C-6})$$

Similarly, after performing the integration with respect to y_2 , Eq. (C-5) is reduced to

$$\text{Im}\Gamma_{\text{II}}^{\text{R}}(\omega + i\delta) = -\frac{\pi V_{\text{dc}}^2 U_{\text{ph}}}{\epsilon_{\text{d}}^2} \left(\prod_{\ell=1,3,4} \int_{-\infty}^{\infty} dy_{\ell} \right) \rho(\mathbf{r}_{ij}, y_1) \rho(\mathbf{r}_{ij}, y_3) \rho(\mathbf{r}_{ij}, y_4) \\ \times \left[\text{th} \left(\frac{y_1}{2T} \right) \frac{\rho(\mathbf{r}_{ij}, y_1 + \omega)}{(-y_1 - y_3)(-y_1 - y_4 + \omega)} - \text{th} \left(\frac{y_3}{2T} \right) \frac{\rho(\mathbf{r}_{ij}, y_3)}{(-y_1 - y_3)(y_3 - y_4 + \omega)} \right. \\ \left. - \text{th} \left(\frac{-y_4 + 2\omega}{2T} \right) \frac{\rho(\mathbf{r}_{ij}, -y_4 + 2\omega)}{(-y_1 - y_4 + \omega)(-y_3 + y_4 - \omega)} \right]. \quad (\text{C-7})$$

By changing the integration variable from y_4 to $y_4 - \omega$, $\text{Im}\Gamma_{\text{I}}^{\text{R}}(\omega + i\delta)$ [E (C-6)] is simplified as

$$\text{Im}\Gamma_{\text{I}}^{\text{R}}(\omega + i\delta) = \frac{2\pi V_{\text{dc}}^2 U_{\text{ph}}}{\epsilon_{\text{d}}^2} \left(\prod_{\ell=2}^4 \int_{-\infty}^{\infty} dy_{\ell} \right) \text{th} \left(\frac{y_4}{2T} \right) \frac{\rho(\mathbf{r}_{ij}, y_2) \rho(\mathbf{r}_{ij}, y_3) \rho(\mathbf{r}_{ij}, y_4 + \omega)}{y_2 + y_4 - \omega} \\ \times \left[\frac{\rho(\mathbf{r}_{ij}, y_4)}{y_3 + y_4} - \frac{\rho(\mathbf{r}_{ij}, -y_4)}{y_3 - y_4} \right]. \quad (\text{C-8})$$

Similarly, by changing the integration variables from $y_1 + \omega$ to y_1 in the first term, and from $-y_3 + \omega$ to y_3 and interchanging $y_1 \rightleftharpoons y_3$ in the second term of Eq. (C-7), $\text{Im}\Gamma_{\text{II}}^{\text{R}}(\omega + i\delta)$ [E (C-7)] is simplified as

$$\text{Im}\Gamma_{\text{II}}^{\text{R}}(\omega + i\delta) = -\frac{\pi V_{\text{dc}}^2 U_{\text{ph}}}{\epsilon_{\text{d}}^2} \left(\prod_{\ell=1,3,4} \int_{-\infty}^{\infty} dy_{\ell} \right) \left\{ \text{th} \left(\frac{y_1}{2T} \right) \left[\frac{\rho(\mathbf{r}_{ij}, y_1 - \omega) \rho(\mathbf{r}_{ij}, y_1) \rho(\mathbf{r}_{ij}, y_3) \rho(\mathbf{r}_{ij}, y_4)}{(-y_1 - y_3 + \omega)(-y_1 - y_4 + 2\omega)} \right. \right. \\ \left. \left. + \frac{\rho(\mathbf{r}_{ij}, y_1 + \omega) \rho(\mathbf{r}_{ij}, -y_1) \rho(\mathbf{r}_{ij}, y_3) \rho(\mathbf{r}_{ij}, y_4)}{(-y_1 - y_3 - \omega)(y_1 - y_4 + 2\omega)} \right] \right. \\ \left. - \text{th} \left(\frac{-y_4 + \omega}{2T} \right) \frac{\rho(\mathbf{r}_{ij}, y_1) \rho(\mathbf{r}_{ij}, y_3) \rho(\mathbf{r}_{ij}, y_4 + \omega) \rho(\mathbf{r}_{ij}, -y_4 + \omega)}{(y_1 + y_4)(y_3 - y_4)} \right\}. \quad (\text{C-9})$$

To perform the integration with respect to y_2 and y_3 in the first term in the brace of Eq. (C-8), we use the spectral representation, Eq. (10), for the Green function G_{c} . Namely, the real part of the retarded Green function of conduction electrons, $G_{\text{c}}^{\text{R}}(\mathbf{r}, \varepsilon)$, is given by

$$G_{\text{c}}^{\text{R}}(\mathbf{r}, \varepsilon) = \int_{-\infty}^{\infty} dy \frac{\rho(\mathbf{r}, y)}{\varepsilon - y}. \quad (\text{C-10})$$

With the use of this relation, Eq. (C-8) is transformed to more compact form as

$$\text{Im}\Gamma_{\text{I}}^{\text{R}}(\omega + i\delta) = \frac{2\pi V_{\text{dc}}^2 U_{\text{ph}}}{\epsilon_{\text{d}}^2} \int_{-\infty}^{\infty} dy_4 \text{th} \left(\frac{y_4}{2T} \right) \rho(\mathbf{r}_{ij}, y_4 + \omega) G_{\text{c}}^{\text{R}}(\mathbf{r}_{ij}, -y_4 + \omega) \\ \times \left[\rho(\mathbf{r}_{ij}, y_4) G_{\text{c}}^{\text{R}}(\mathbf{r}_{ij}, -y_4) - \rho(\mathbf{r}_{ij}, -y_4) G_{\text{c}}^{\text{R}}(\mathbf{r}_{ij}, y_4) \right]. \quad (\text{C-11})$$

Similarly, Eq. (C-9) is transformed to the following from

$$\text{Im}\Gamma_{\text{II}}^{\text{R}}(\omega + i\delta) = -\frac{\pi V_{\text{dc}}^2 U_{\text{ph}}}{\epsilon_{\text{d}}^2} \left\{ \int_{-\infty}^{\infty} dy_1 \text{th} \left(\frac{y_1}{2T} \right) \right. \\ \left[\rho(\mathbf{r}_{ij}, y_1 - \omega) \rho(\mathbf{r}_{ij}, y_1) G_{\text{c}}^{\text{R}}(\mathbf{r}_{ij}, -y_1 + \omega) G_{\text{c}}^{\text{R}}(\mathbf{r}_{ij}, -y_1 + 2\omega) \right. \\ \left. + \rho(\mathbf{r}_{ij}, y_1 + \omega) \rho(\mathbf{r}_{ij}, -y_1) G_{\text{c}}^{\text{R}}(\mathbf{r}_{ij}, -y_1 - \omega) G_{\text{c}}^{\text{R}}(\mathbf{r}_{ij}, y_1 + 2\omega) \right] \\ \left. + \int_{-\infty}^{\infty} dy_1 \text{th} \left(\frac{y_4 - \omega}{2T} \right) \left[\rho(\mathbf{r}_{ij}, y_4 + \omega) \rho(\mathbf{r}_{ij}, -y_4 + \omega) G_{\text{c}}^{\text{R}}(\mathbf{r}_{ij}, -y_4) G_{\text{c}}^{\text{R}}(\mathbf{r}_{ij}, y_4) \right] \right\}. \quad (\text{C-12})$$

Changing the integration variables from y_1 to $y_1 - \omega$ and from y_1 to $-y_1 + \omega$ in the first and second term in the bracket of Eq. (C-12), the first term in the brace of Eq. (C-12) is transformed to

$$-\frac{\pi V_{\text{dc}}^2 U_{\text{ph}}}{\epsilon_{\text{d}}^2} \int_{-\infty}^{\infty} dy_1 \text{th} \left(\frac{y_1 + \omega}{2T} \right) \left[\rho(\mathbf{r}_{ij}, y_1) G_{\text{c}}^{\text{R}}(\mathbf{r}_{ij}, -y_1 + \omega) \rho(\mathbf{r}_{ij}, y_1 + \omega) G_{\text{c}}^{\text{R}}(\mathbf{r}_{ij}, -y_1) \right. \\ \left. - \rho(\mathbf{r}_{ij}, -y_1) G_{\text{c}}^{\text{R}}(\mathbf{r}_{ij}, -y_1 + \omega) \rho(\mathbf{r}_{ij}, y_1 + \omega) G_{\text{c}}^{\text{R}}(\mathbf{r}_{ij}, y_1) \right]. \quad (\text{C-13})$$

By changing the integration variable from y_4 to y_1 in Eq. (C-11), $\text{Im}\Gamma_{\text{I}}^{\text{R}}(\omega + i\delta)$ is transformed to

$$\begin{aligned} \text{Im}\Gamma_{\text{I}}^{\text{R}}(\omega + i\delta) &= \frac{2\pi V_{\text{dc}}^2 U_{\text{ph}}}{\epsilon_{\text{d}}^2} \int_{-\infty}^{\infty} dy_1 \text{th}\left(\frac{y_1}{2T}\right) \rho(\mathbf{r}_{ij}, y_1 + \omega) G_{\text{c}}^{\text{R}}(\mathbf{r}_{ij}, -y_1 + \omega) \\ &\quad \times \left[\rho(\mathbf{r}_{ij}, y_1) G_{\text{c}}^{\text{R}}(\mathbf{r}_{ij}, -y_1) - \rho(\mathbf{r}_{ij}, -y_1) G_{\text{c}}^{\text{R}}(\mathbf{r}_{ij}, y_1) \right]. \end{aligned} \quad (\text{C-14})$$

It is easy to see that the expression of integrand in Eq. (C-13) and Eq. (C-14) are same except for the difference of argument x in $\text{th}(x)$. Since the $\text{Im}\Gamma_{\text{II}}(\omega + i\delta)$ arises twice from the integration along $\text{Im}z = \pm\omega_{\text{v}}$, the ω -linear term in twice of Eq. (C-13) and that in Eq. (C-14) cancels with each other in the low temperature region, $T \ll \epsilon_{\text{F}}$, where $\{\text{th}[(y_1 + \omega)/2T] - \text{th}(y_1/2T)\} \approx 2\omega\delta(y_1)$ so that the expression in the bracket in Eq. (C-14) technically vanishes. Therefore, $2\text{Im}\Gamma_{\text{II}}(\omega + i\delta) + \text{Im}\Gamma_{\text{I}}(\omega + i\delta)$ is given by twice of the second term in the brace of Eq. (C-12). Namely, $\text{Im}\tilde{\Gamma}_{\text{ph}}^{\text{R}}(\omega + i\delta) \equiv 2\text{Im}\Gamma_{\text{II}}^{\text{R}}(\omega + i\delta) + \text{Im}\Gamma_{\text{I}}^{\text{R}}(\omega + i\delta)$ is given by

$$\begin{aligned} \text{Im}\tilde{\Gamma}_{\text{ph}}^{\text{R}}(\omega + i\delta) &= -\frac{2\pi V_{\text{dc}}^2 U_{\text{ph}}}{\epsilon_{\text{d}}^2} \int_{-\infty}^{\infty} dy_4 \text{th}\left(\frac{y_4 - \omega}{2T}\right) \\ &\quad \times \left[\rho(\mathbf{r}_{ij}, y_4 + \omega) \rho(\mathbf{r}_{ij}, -y_4 + \omega) G_{\text{c}}^{\text{R}}(\mathbf{r}_{ij}, -y_4) G_{\text{c}}^{\text{R}}(\mathbf{r}_{ij}, y_4) \right] \\ &= -\frac{2\pi V_{\text{dc}}^2 U_{\text{ph}}}{\epsilon_{\text{d}}^2} \int_{-\infty}^{\infty} dy_4 \left[\text{th}\left(\frac{y_4 - \omega}{2T}\right) - \text{th}\frac{y_4}{2T} \right] \\ &\quad \times \left[\rho(\mathbf{r}_{ij}, y_4 + \omega) \rho(\mathbf{r}_{ij}, -y_4 + \omega) G_{\text{c}}^{\text{R}}(\mathbf{r}_{ij}, -y_4) G_{\text{c}}^{\text{R}}(\mathbf{r}_{ij}, y_4) \right], \end{aligned} \quad (\text{C-15})$$

where, in deriving the second equality, we have used the fact that the function in the bracket is an even function in y_4 so that the term including $\text{th}(y_4/2T)$ vanishes.

Appendix D: Case of direct overlap of electrons between Tl and Te sites

In the case where the localized state at Tl site extends to the adjacent Te site, the relaxation function Γ' , corresponding to $\tilde{\Gamma}_{\text{ph}}$ defined by Eq. (C-1), is derived from the Feynman diagram shown in Fig. D-1 and its vertical inversion. Its analytic expression is given by

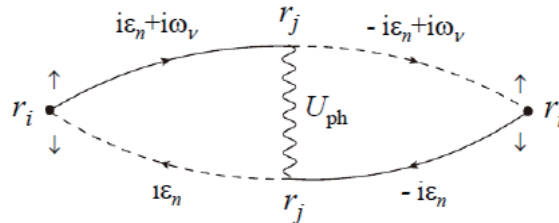


Fig. D-1. Feynman diagram giving the NMR longitudinal relaxation rates $1/T_1T$ at Te (\mathbf{r}_i) site, in the case where 6s electron at Tl (\mathbf{r}_j) site extends to the Te (\mathbf{r}_i) site.

$$\Gamma'(i\omega_\nu) = 2U_{\text{ph}}T \sum_{\varepsilon_n} G_c(\mathbf{r}_{ij}, i\varepsilon_n + i\omega_\nu) G_c(\mathbf{r}_{ij}, -i\varepsilon_n) \times G_d(-i\varepsilon_n + i\omega_\nu) G_d(i\varepsilon_n) \quad (\text{D}\cdot 1)$$

Instead of Eq. (C.1), we obtain.

$$\Gamma'(i\omega_\nu) = 2U_{\text{ph}}T \sum_{\varepsilon_n} \left(\prod_{\ell=2}^3 \int_{-\infty}^{\infty} dy_\ell \right) \frac{\rho(\mathbf{r}_{ij}, y_2)}{i\varepsilon_n + i\omega_\nu - y_2} \frac{\rho(\mathbf{r}_{ij}, y_3)}{-i\varepsilon_n - y_3} \frac{1}{i\varepsilon_n - \epsilon_d} \frac{1}{-i\varepsilon_n + i\omega_\nu - \epsilon_d} \quad (\text{D}\cdot 2)$$

Note that we have not approximated $G_d(-i\varepsilon_n)G_d(i\varepsilon_n)$ by $1/\epsilon_d^2$. The summation in Eq. (D.2) with respect to ε_n is performed in a standard way by transforming the summation to the integration along the axes $\text{Im}z = 0$ and $\text{Im}z = \pm\omega_\nu$ on z -plane, where one is just above these axes and another is just below in the counter direction. The result is

$$\Gamma'(i\omega_\nu) = U_{\text{ph}} \left(\prod_{\ell=2}^3 \int_{-\infty}^{\infty} dy_\ell \right) \rho(\mathbf{r}_{ij}, y_2) \rho(\mathbf{r}_{ij}, y_3) \times \left\{ \frac{1}{y_3 + \epsilon_d} \left[\text{th}\left(\frac{y_3}{2T}\right) \frac{1}{-y_2 - y_3 + i\omega_\nu} \frac{1}{y_3 - \epsilon_d + i\omega_\nu} + \text{th}\left(\frac{\epsilon_d}{2T}\right) \frac{1}{\epsilon_d - y_2 + i\omega_\nu} \frac{1}{-2\epsilon_d + i\omega_\nu} \right] + \frac{1}{y_2 + \epsilon_d - 2i\omega_\nu} \left[\text{th}\left(\frac{y_2}{2T}\right) \frac{1}{-y_2 - y_3 + i\omega_\nu} \frac{1}{y_2 - \epsilon_d - i\omega_\nu} + \text{th}\left(\frac{\epsilon_d}{2T}\right) \frac{1}{\epsilon_d - y_3 - i\omega_\nu} \frac{1}{-2\epsilon_d + i\omega_\nu} \right] \right\}$$

After analytic continuation, $i\omega_\nu \rightarrow \omega + i\delta$ in Eq. (D.3), and taking an imaginary part, we obtain

$$\begin{aligned} \text{Im}\Gamma'^{\text{R}}(\omega + i\delta) &= -\pi U_{\text{ph}} \left(\prod_{\ell=2}^3 \int_{-\infty}^{\infty} dy_\ell \right) \rho(\mathbf{r}_{ij}, y_2) \rho(\mathbf{r}_{ij}, y_3) \frac{1}{y_3 + \epsilon_d} \\ &\quad \times \left\{ \text{th}\left(\frac{y_3}{2T}\right) \left[\frac{\delta(y_3 - \epsilon_d + \omega)}{-y_2 - y_3 + \omega} + \frac{\delta(y_2 + y_3 - \omega)}{y_3 - \epsilon_d + \omega} \right] \right. \\ &\quad \left. + \text{th}\left(\frac{\epsilon_d}{2T}\right) \left[\frac{\delta(-2\epsilon_d + \omega)}{\epsilon_d - y_2 + \omega} + \frac{\delta(\epsilon_d - y_2 + \omega)}{-2\epsilon_d + \omega} \right] \right\} \\ &+ \pi U_{\text{ph}} \left(\prod_{\ell=2}^3 \int_{-\infty}^{\infty} dy_\ell \right) \rho(\mathbf{r}_{ij}, y_2) \rho(\mathbf{r}_{ij}, y_3) \\ &\quad \times \left\{ \text{th}\left(\frac{y_2}{2T}\right) \frac{1}{-y_2 - \epsilon_d + 2\omega} \left[\frac{\delta(y_2 + y_3 - \omega)}{y_2 - \epsilon_d - \omega} + \frac{\delta(y_2 - \epsilon_d - \omega)}{y_2 + y_3 - \omega} \right] \right. \\ &\quad - \text{th}\left(\frac{y_2}{2T}\right) \frac{\delta(y_2 + \epsilon_d - 2\omega)}{(y_2 + y_3 - \omega)(y_2 - \epsilon_d - \omega)} \\ &\quad \left. + \text{th}\left(\frac{\epsilon_d}{2T}\right) \frac{1}{-2\epsilon_d + \omega} \left[\frac{\delta(y_2 + \epsilon_d - 2\omega)}{\epsilon_d - y_3 - \omega} + \frac{\delta(y_3 - \epsilon_d + \omega)}{\epsilon_d + y_2 - 2\omega} \right] \right\} \quad (\text{D}\cdot 4) \end{aligned}$$

Performing the integration with respect to y_2 or y_3 , Eq. (D.4) is reduced to

$$\text{Im}\Gamma'^{\text{R}}(\omega + i\delta) = -\pi U_{\text{ph}} \int_{-\infty}^{\infty} dy_2 \rho(\mathbf{r}_{ij}, y_2)$$

$$\begin{aligned}
& \times \left\{ \left[\text{th} \left(\frac{\epsilon_d - \omega}{2T} \right) - \text{th} \left(\frac{\epsilon_d}{2T} \right) \right] \frac{\rho(\mathbf{r}_{ij}, \epsilon_d - \omega)}{(-\epsilon_d - y_2 + 2\omega)(2\epsilon_d - \omega)} \right. \\
& + \left[\text{th} \left(\frac{\epsilon_d - 2\omega}{2T} \right) - \text{th} \left(\frac{\epsilon_d}{2T} \right) \right] \frac{\rho(\mathbf{r}_{ij}, -\epsilon_d + 2\omega)}{(-\epsilon_d + y_2 + \omega)(2\epsilon_d - \omega)} \\
& - \left[\text{th} \left(\frac{y_2 - \omega}{2T} \right) - \text{th} \left(\frac{y_2}{2T} \right) \right] \frac{\rho(\mathbf{r}_{ij}, -y_2 + \omega)}{(-y_2 - \epsilon_d + 2\omega)(-y_2 + \epsilon_d + \omega)} \\
& \left. + \left[\text{th} \left(\frac{\epsilon_d}{2T} \right) - \text{th} \left(\frac{\epsilon_d + \omega}{2T} \right) \right] \frac{\rho(\mathbf{r}_{ij}, \epsilon_d + \omega)}{(y_2 + \epsilon_d)(-2\epsilon_d + \omega)} \right\}. \quad (\text{D}\cdot 5)
\end{aligned}$$

The first and fourth terms give only vanishing contribution because $\rho(\mathbf{r}_{ij}, \epsilon_d)$ [Eq. (11)] are vanishing in the present case $\epsilon_d < -\epsilon_F$. The second term also gives vanishing contribution because $\{\text{th}[(\epsilon_d - 2\omega)/2T] - \text{th}(\epsilon_d/2T)\}$ is vanishing if the ϵ_d is located well below the bottom of the conduction band (in the hole picture). Therefore, Eq. (D-5) is finally reduced to

$$\text{Im}\Gamma'^{\text{R}}(\omega + i\delta) = \pi U_{\text{ph}} \int_{-\infty}^{\infty} dy_2 \left[\text{th} \left(\frac{y_2 - \omega}{2T} \right) - \text{th} \frac{y_2}{2T} \right] \frac{\rho(\mathbf{r}_{ij}, y_2)\rho(\mathbf{r}_{ij}, -y_2 + \omega)}{(-y_2 - \epsilon_d + 2\omega)(-y_2 + \epsilon_d + \omega)}. \quad (\text{D}\cdot 6)$$

Then, up to the linear term in ω , $\text{Im}\Gamma'(\omega + i\delta)$ is given as

$$\text{Im}\Gamma'^{\text{R}}(\omega + i\delta) \approx -\omega \pi U_{\text{ph}} \int_{-\infty}^{\infty} dy_2 \frac{\partial \text{th} \left(\frac{y_2}{2T} \right)}{\partial y_2} \frac{\rho(\mathbf{r}_{ij}, y_2)\rho(\mathbf{r}_{ij}, -y_2)}{(-y_2 - \epsilon_d)(-y_2 + \epsilon_d)}. \quad (\text{D}\cdot 7)$$

Considering that $\rho(\mathbf{r}_{ij}, y_2)\rho(\mathbf{r}_{ij}, -y_2 + \omega)$ with $\omega \approx 0$ is vanishing at $|y_2| > \epsilon_F$ and $|\epsilon_d| \gg \epsilon_F$, the expression [Eq. (D-7)] is further simplified as

$$\begin{aligned}
\text{Im}\Gamma'^{\text{R}}(\omega + i\delta) & \approx \omega \frac{\pi U_{\text{ph}}}{\epsilon_d^2} \int_{-\infty}^{\infty} dy_2 \frac{\partial \text{th} \left(\frac{y_2}{2T} \right)}{\partial y_2} \rho(\mathbf{r}_{ij}, y_2)\rho(\mathbf{r}_{ij}, -y_2) \\
& \approx \omega \frac{2\pi U_{\text{ph}}}{\epsilon_d^2} \left[\rho(\mathbf{r}_{ij}, 0) \right]^2. \quad (\text{D}\cdot 8)
\end{aligned}$$

If $G_d(i\epsilon_n + i\omega_\nu)G_d(-i\epsilon_n)$ in Eq. (D-1) is approximated by $1/\epsilon_d^2$ as in Eq. (C-1), the relaxation function $\Gamma''(i\omega_\nu)$ is easily calculated as follows:

$$\begin{aligned}
\Gamma''^{\text{R}}(i\omega_\nu) & = \frac{2U_{\text{ph}}}{\epsilon_d^2} T \sum_{\epsilon_n} G_c(\mathbf{r}_{ij}, i\epsilon_n + i\omega_\nu) G_c(\mathbf{r}_{ij}, -i\epsilon_n) \\
& = \frac{2U_{\text{ph}}}{\epsilon_d^2} T \sum_{\epsilon_n} \left(\prod_{\ell=2}^3 \int_{-\infty}^{\infty} dy_\ell \right) \frac{\rho(\mathbf{r}_{ij}, y_2)}{i\epsilon_n + i\omega_\nu - y_2} \frac{\rho(\mathbf{r}_{ij}, y_3)}{-i\epsilon_n - y_3} \\
& = \frac{2U_{\text{ph}}}{\epsilon_d^2} \left(\prod_{\ell=2}^3 \int_{-\infty}^{\infty} dy_\ell \right) \frac{1}{2} \left(\text{th} \frac{y_2}{2T} + \text{th} \frac{y_3}{2T} \right) \frac{\rho(\mathbf{r}_{ij}, y_2)\rho(\mathbf{r}_{ij}, y_3)}{-y_2 - y_3 + i\omega_\nu} \quad (\text{D}\cdot 9)
\end{aligned}$$

After analytic continuation, $i\omega_\nu \rightarrow \omega + i\delta$ in Eq. (D-9), and performing an integration with respect to y_3 , $\text{Im}\Gamma''^{\text{R}}(\omega + i\delta)$ is reduced to

$$\text{Im}\Gamma''^{\text{R}}(\omega + i\delta) = \frac{2\pi U_{\text{ph}}}{\epsilon_d^2} \int_{-\infty}^{\infty} dy_2 \frac{1}{2} \left[\text{th} \frac{y_2}{2T} - \text{th} \left(\frac{y_2 - \omega}{2T} \right) \right] \rho(\mathbf{r}_{ij}, y_2)\rho(\mathbf{r}_{ij}, -y_2 + \omega). \quad (\text{D}\cdot 10)$$

Then, up to the linear order in ω , $\text{Im}\Gamma''(\omega + i\delta)$ is given as

$$\begin{aligned} \text{Im}\Gamma''^{\text{R}}(\omega + i\delta) &\approx \omega \frac{\pi U_{\text{ph}}}{\epsilon_{\text{d}}^2} \int_{-\infty}^{\infty} dy_2 \frac{\partial \text{th}\left(\frac{y_2}{2T}\right)}{\partial y_2} \rho(\mathbf{r}_{ij}, y_2) \rho(\mathbf{r}_{ij}, -y_2) \\ &\approx \omega \frac{2\pi U_{\text{ph}}}{\epsilon_{\text{d}}^2} [\rho(\mathbf{r}_{ij}, 0)]^2, \end{aligned} \quad (\text{D}\cdot 11)$$

which is the same as the expression [Eq. (D-8)]. This justifies the approximation $G_{\text{d}}(i\epsilon_n + i\omega_\nu)G_{\text{d}}(-i\epsilon_n) \approx 1/\epsilon_{\text{d}}^2$ in Eq. (D-1), which in turn justifies the same approximation adopted in Eq. (C-1). A physical basis of this justification is that the $\text{Im}\Gamma^{\text{R}}(\omega + i\delta)$ arises only from the low energy processes associated with conduction electrons described by $G_{\text{c}}(\mathbf{r}_{ij}, i\epsilon_n + i\omega_\nu)$ and $G_{\text{c}}(\mathbf{r}_{ij}, -i\epsilon_n)$ in Eq. (D-1), so that the same approximation is expected to remain valid also in the calculation of $\text{Im}\tilde{\Gamma}_{\text{ph}}^{\text{R}}(\omega + i\delta)$ performed in Appendix .

In the limit $k_{\text{F}}|\mathbf{r}_{ij}| \ll 1$, with the use of asymptotic form of $\rho(\mathbf{r}, y)$ [Eq. (12)], Eq. (D-11) is estimated as

$$\text{Im}\Gamma''^{\text{R}}(\omega + i\delta) \approx \omega \frac{2\pi N_{\text{F}}^2}{\epsilon_{\text{d}}^2} e^{-(|\mathbf{r}_{ij}|/\ell)} U_{\text{ph}} + O(\omega^2). \quad (\text{D}\cdot 12)$$

Then, the NMR relaxation rate $1/T_1 T$ is given by

$$\frac{1}{T_1 T} = A^2 \frac{2\pi N_{\text{F}}^2}{\epsilon_{\text{d}}^2} e^{-(|\mathbf{r}_{ij}|/\ell)} U_{\text{ph}}. \quad (\text{D}\cdot 13)$$

Appendix E: Real-Part of Retarded Green Function of Conduction Electrons

In this Appendix, we derive an analytic form of $G_{\text{c}}^{\text{R}}(\mathbf{r}, \epsilon)$ [Eq. (17)] in the limit $k_{\text{F}}r \ll 1$, where $G_{\text{c}}^{\text{R}}(\mathbf{r}, \epsilon)$ is approximated by

$$G_{\text{c}}^{\text{R}}(\mathbf{r}, \epsilon) \approx -\frac{mk_{\text{F}}}{2\pi^2} e^{-(r/2\ell)} \frac{1}{\sqrt{\epsilon_{\text{F}}}} \int_{-\epsilon_{\text{F}}}^{\epsilon_{\text{c}}} dy \frac{\sqrt{y + \epsilon_{\text{F}}}}{y - \epsilon}. \quad (\text{E}\cdot 1)$$

Integration with respect to y is performed by elementary integral leading to the following results. In the case $\epsilon + \epsilon_{\text{F}} > 0$,

$$\int_{-\epsilon_{\text{F}}}^{\epsilon_{\text{c}}} dy \frac{\sqrt{y + \epsilon_{\text{F}}}}{y - \epsilon} = 2\sqrt{\epsilon_{\text{c}} + \epsilon_{\text{F}}} + \sqrt{\epsilon + \epsilon_{\text{F}}} \log \left| \frac{\sqrt{\epsilon_{\text{c}} + \epsilon_{\text{F}}} - \sqrt{\epsilon + \epsilon_{\text{F}}}}{\sqrt{\epsilon_{\text{c}} + \epsilon_{\text{F}}} + \sqrt{\epsilon + \epsilon_{\text{F}}}} \right|, \quad (\text{E}\cdot 2)$$

while in the case $\epsilon + \epsilon_{\text{F}} < 0$,

$$\int_{-\epsilon_{\text{F}}}^{\epsilon_{\text{c}}} dy \frac{\sqrt{y + \epsilon_{\text{F}}}}{y - \epsilon} = 2\sqrt{\epsilon_{\text{c}} + \epsilon_{\text{F}}} - 2\sqrt{-\epsilon - \epsilon_{\text{F}}} \tan^{-1} \frac{\sqrt{\epsilon_{\text{c}} + \epsilon_{\text{F}}}}{\sqrt{-\epsilon - \epsilon_{\text{F}}}}. \quad (\text{E}\cdot 3)$$

Appendix F: Calculation of $J(k_{\text{F}}r)$ in the limit $k_{\text{F}}r \gg 1$

In this Appendix, we derive an asymptotic form of $J(k_{\text{F}}r)$, Eq. (19), in the limit $k_{\text{F}}r \gg 1$. The integration in Eq. (19) with respect to y , which is denoted by K , is transformed, by changing the integration variable from y to $u \equiv \sqrt{(y/\epsilon_{\text{F}}) + 1}$ and defining $\Lambda \equiv \sqrt{(\epsilon_{\text{c}}/\epsilon_{\text{F}}) + 1}$, as follows:

$$K = \int_0^\Lambda du \frac{2u}{(u+1)(u-1)} \sin[(k_{\text{F}}r)u]$$

$$= \text{Im} \left[\int_0^\Lambda du \frac{2u}{(u+1)(u-1)} e^{i(k_{\text{F}}r)u} \right], \quad (\text{F}\cdot 1)$$

where the integration with respect to u is the principal integration for avoiding the singularity around $u = 1$.

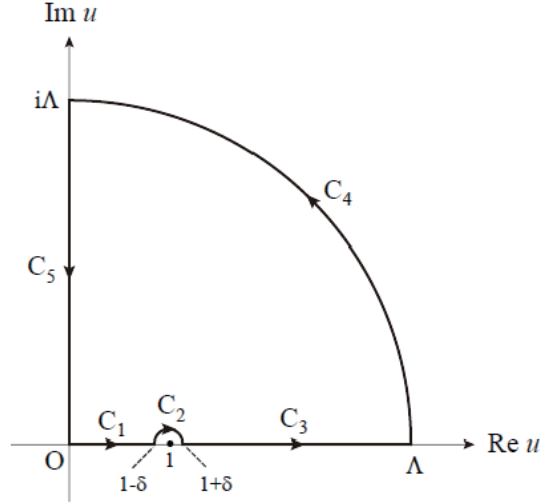


Fig. F-1. Path of contour integration in Eq. (F-1) in the complex- u plane.

Let us define K_i ($i = 1 \sim 5$) by integration with respect complex u along the path C_i shown in Fig. F-1 as

$$K_i \equiv \int_{C_i} du \frac{2u}{(u+1)(u-1)} e^{i(k_{\text{F}}r)u}. \quad (\text{F}\cdot 2)$$

An infinitesimally small positive number δ in Fig. F-1 will be tended to zero after calculations. $\lim_{\delta \rightarrow 0} [K_1(\delta) + K_3(\delta)]$ is the same as the principal integration in Eq. (F-1). The integration along C_2 , a semicircle with the radius δ , is performed in the limit $\delta \rightarrow 0$ as

$$\begin{aligned} K_2 &= \int_\pi^0 d(\delta e^{i\varphi}) \frac{2(1 + \delta e^{i\varphi})}{(2 + \delta e^{i\varphi}) \delta e^{i\varphi}} e^{i(k_{\text{F}}r)(1 + \delta e^{i\varphi})} \\ &\approx i \int_\pi^0 d\varphi e^{i(k_{\text{F}}r)} = -i \pi \cos(k_{\text{F}}r) + \pi \sin(k_{\text{F}}r). \end{aligned} \quad (\text{F}\cdot 3)$$

It is easy to see that $K_5(\Lambda)$ is real and finite number. The integration along C_4 , a semicircle with the radius Λ , is performed as

$$\begin{aligned} K_4(\Lambda) &= \int_0^{\pi/2} d(\Lambda e^{i\theta}) \frac{2\Lambda e^{i\theta}}{\Lambda^2 e^{2i\theta} - 1} e^{[i(k_{\text{F}}r)\Lambda e^{i\theta}]} \\ &= i \int_0^{\pi/2} d\theta \frac{2\Lambda^2 e^{2i\theta}}{\Lambda^2 e^{2i\theta} - 1} e^{i(k_{\text{F}}r)\Lambda \cos \theta} e^{-(k_{\text{F}}r)\Lambda \sin \theta}. \end{aligned} \quad (\text{F}\cdot 4)$$

It is shown by a standard way of calculus that $K_4(\Lambda)$ vanishes in proportion to $1/(k_{\text{F}}r)$ in the limit

$k_{\text{F}}r \gg 1$.

Therefore, Eq. (F.1) is transformed in the limit $k_{\text{F}}r \gg 1$ as follows:

$$\begin{aligned} K &= \lim_{\delta \rightarrow 0} \text{Im}[K_1(\delta) + K_3(\delta)] \\ &= \lim_{\delta \rightarrow 0} \text{Im} \left\{ [K_1(\delta) + K_3(\delta) + K_2(\delta) + K_4 + K_5] \right. \\ &\quad \left. - [K_2(\delta) + K_4 + K_5] \right\} \end{aligned} \quad (\text{F}\cdot 5)$$

$$= - \lim_{\delta \rightarrow 0} \text{Im} [K_2(\delta) + K_4 + K_5] \quad (\text{F}\cdot 6)$$

$$\approx - \lim_{\delta \rightarrow 0} \text{Im} K_2(\delta) = \pi \cos(k_{\text{F}}r). \quad (\text{F}\cdot 7)$$

In deriving Eq. (F.6) from Eq. (F.5), we have used the fact that the contour integration in the complex- u plane along the path shown in Fig. F.1 vanishes because the integrand is an analytic function in the domain encircled by the contour. In deriving Eq. (F.7) from Eq. (F.6), we have used Eq. (F.3).

As a result, $J(k_{\text{F}}r)$ [Eq. (19)] in the limit $k_{\text{F}}r \gg 1$ is given by

$$J(k_{\text{F}}r) \approx \frac{1}{k_{\text{F}}r} \pi \cos(k_{\text{F}}r). \quad (\text{F}\cdot 8)$$

Appendix G: Poorman's Scaling Analysis for U_{ph} and U_{dc}

In this Appendix, we perform the poorman's scaling analysis for the pair-hopping interaction U_{ph} and the inter-orbital interaction U_{dc} to investigate renormalization effect on these interaction. As discussed in Appendix, in the mapped world, U_{ph} and U_{dc} correspond to $J_{\perp}/2$ and $J_z/4$ in the anisotropic s-d model. The evolution equations for these dimensionless coupling constants, $y_{\perp} \equiv J_{\perp}N_{\text{F}}$ and $y_z \equiv J_zN_{\text{F}}$ are given as follows:¹⁹⁾

$$\frac{dy_{\perp}}{dx} = -y_{\perp}y_z, \quad (\text{G}\cdot 1)$$

$$\frac{dy_z}{dx} = -y_{\perp}^2, \quad (\text{G}\cdot 2)$$

where $x \equiv \log(E_c/E_c^0)$ with E_c and E_c^0 being the renormalized and bare bandwidths, respectively. It is well known that $y_{\perp}^2 - y_z^2 = \text{const.} \equiv C$. Substituting $y_{\perp}^2 = y_z^2 + C$ into Eq. (G.2), the evolution equation of y_z [Eq. (G.2)] is reduced to

$$\frac{dy_z}{dx} = -(y_z^2 + C). \quad (\text{G}\cdot 3)$$

The solution of this differential equation is easily solved: In the case $C \equiv a^2 > 0$,

$$y_z(x) = \frac{y_z^0 - a \tan(ax)}{1 + \frac{y_z^0}{a} \tan(ax)}, \quad (\text{G}\cdot 4)$$

where y_z^0 is the initial value of y_z at $x = 0$. Similarly, in the case $C \equiv -b^2 < 0$, the solution is given as

$$y_z(x) = \frac{y_z^0 + b \tanh(bx)}{1 + \frac{y_z^0}{b} \tanh(bx)}. \quad (\text{G}\cdot 5)$$

In the high temperature region, $T \gtrsim T_K$, where $|x| \ll 1$, both $y_z(x)$ [Eq. (G-4)] and $y_z(x)$ [Eq. (G-5)] are expressed as

$$y_z(x) \approx y_z^0 - (y_\perp^0)^2 x + \dots. \quad (\text{G}\cdot 6)$$

With the use of this approximate expression, that for y_\perp is easily obtained in the following form

$$y_\perp(x) \approx y_\perp^0 - y_\perp^0 y_z^0 x + \dots. \quad (\text{G}\cdot 7)$$

Therefore, in the high temperature region $T \gtrsim T_K$, temperature dependence of $U_{\text{ph}} = (J_\perp/2)$ and $U_{\text{dc}} = (J_z/4)$ are given as follows:

$$U_{\text{ph}}(T) = \frac{1}{2N_F} y_\perp \left(\log \frac{T}{E_c^0} \right) \approx \frac{1}{2} \left[2U_{\text{ph}}^0 - 8N_F U_{\text{ph}} U_{\text{dc}}^0 \log \frac{T}{E_c^0} \right], \quad (\text{G}\cdot 8)$$

$$U_{\text{dc}}(T) = \frac{1}{4N_F} y_z \left(\log \frac{T}{E_c^0} \right) \approx \frac{1}{4} \left[4U_{\text{dc}}^0 - N_F (2U_{\text{ph}}^0)^2 \log \frac{T}{E_c^0} \right], \quad (\text{G}\cdot 9)$$

where U_{ph}^0 and U_{dc}^0 are bare couplings. Namely, both $U_{\text{ph}}(T)$ and $U_{\text{dc}}(T)$ exhibit logarithmic increase toward $T = T_K$ at which $y_\perp(x)$ and $y_z(x)$ diverges at the level of approximation of the poorman's scaling.¹⁹⁾

On the other hand, both $y_\perp(E)$ and $y_z(E)$ diverge toward $E = T_K$ as

$$y_\perp(E) = \frac{y_\perp(0)}{1 + y_\perp(0) \log \frac{E}{E_c^0}} = \frac{1}{\log \frac{E}{T_K}} \approx y_z(E), \quad (\text{G}\cdot 10)$$

where T_K is given by the solution for the case $C = 0$ as $T_K = E_c^0 e^{-y_\perp(0)}$ or $[1 + y_\perp(0) \log(T_K/E_c^0)] = 0$. Of course, this divergence at $E = T_K$ is an artifact due to the one-loop order approximation, but true divergence occurs in the limit $E \ll T_K$. Namely, the expression [Eq.(G-10)] is not valid very near at $E = T_K$ while it gives growing tendency of $y_\perp(E)$ and $y_z(E)$ toward $E = T_K$

References

- 1) Y. Matsushita, H. Bluhm, T. H. Geballe, and I. R. Fisher, Phys. Rev. Lett. **94**, 157002 (2005).
- 2) R. D. Shannon, Acta Cryst. A **32**, 751 (1976).
- 3) M. Dzero and J. Schmalian, Phys. Rev. Lett. **94**, 157003 (2005).
- 4) A. Taraphder and P. Coleman, Phys. Rev. Lett. **66**, 2814 (1991).
- 5) H. Matsuura and K. Miyake, J. Phys. Soc. Jpn. **81**, 113705 (2012).
- 6) P. W. Anderson, Phys. Rev. Lett. **34**, 953 (1975).
- 7) H. Katayama-Yoshida and A. Zunger, Phys. Rev. Lett. **55**, 1618 (1985).
- 8) I. Hase and T. Yanagisawa, Phys. Rev. B **76**, 174103 (2007).
- 9) W. A. Harrison, Phys. Rev. B **74**, 245128 (2006).
- 10) A. C. Hewson and D. Meyer, J. Phys. Condens. Matter **14**, 427 (2002).
- 11) T. Hotta, J. Phys. Soc. Jpn. **76**, 084702 (2007).
- 12) R. Shinzaki, J. Nasu, and A. Koga, Phys Rev B **97**, 125130 (2018).
- 13) H. Mukuda, T. Matsumura, S. Maki, M. Yashima, Y. Kitaoka, H. Murakami, K. Miyake, P. Giraldo-Gallo, T. H. Geballe, and I. R. Fisher, J. Phys. Soc. Jpn. **87** 023706 (2018).
- 14) T. Moriya, J. Phys. Soc. Jpn. **18**, 516 (1963).
- 15) K. Maki, Prog. Theor. Phys. **40**, 193 (1968).
- 16) R. S. Thompson, Phys. Rev. B **1**, 327 (1970).
- 17) L. G. Aslamosov and A. I. Larkin, Phys. Lett. A **26**, 238 (1968).
- 18) S. Tanikawa, H. Matsuura, and K. Miyake, J. Phys. Soc. Jpn. **78**, 034707 (2009).
- 19) P. W. Anderson, J. Phys. C **3**, 2436 (1970).
- 20) R. Horikawa, M. Yashima, T. Matsumura, S. Maki, H. Mukuda, K. Miyake, H. Murakami, P. Walmsley, P. Giraldo-Gallo, T. H. Geballe, and I. R. Fisher, JPS Conf. Proc. **30** 011126 (2020).
- 21) K. Miyake and S. Watanabe, Phys. Rev. B **98**, 075125 (2018).
- 22) H. Shiba: Prog. Theor. Phys. **48**, 2171 (1972).
- 23) R. Micnas, J. Ranninger, and S. Robaszkiewicz, Rev. Mod. Phys. **62**, 113 (1990).
- 24) A. A. Abrikosov, L. P. Gor'kov, and I. Ye. Dzyaloshinskii, *Quantum Field Theoretical Methods in Statistical Physics* (Pergamon, Oxford, U.K., 1965) 2nd ed., Sect. 39.2.
- 25) K. Yosida, Phys. Rev. **147**, 223 (1966); Prog. Theor. Phys. **36**, 875 (1966).
- 26) A. Yoshimori and K. Yosida, Prog. Theor. Phys. **39**, 1413 (1968).
- 27) P. Nozières, J. Low Temp. Phys. **17**, 31 (1974).
- 28) H. Shiba, Prog. Theor. Phys. **54**, 967 (1975).
- 29) S. Yotsuhashi, K. Miyake, and H. Kusunose, Physica B **312-313**, 100 (2002).
- 30) S. Yotsuhashi, K. Miyake, and H. Kusunose, J. Phys. Soc Jpn. **85**, 034719 (2016).
- 31) A. A. Abrikosov, L. P. Gor'kov, and I. Ye. Dzyaloshinskii, *Quantum Field Theoretical Methods in Statistical Physics* (Pergamon, Oxford, U.K., 1965) 2nd ed., Sect. 17. See Eq. (17.19).
- 32) H. Mukuda, private communication.
- 33) See, e.g., K. Ishida, Y. Kitaoka, and K. Asayama, J. Phys. Soc. Jpn. **58**, 36 (1989).